

Cover Page



Universiteit Leiden



The handle <http://hdl.handle.net/1887/43190> holds various files of this Leiden University dissertation.

Author: Raeven, R.H.M.

Title: Systems vaccinology : molecular signatures of immunity to Bordetella pertussis

Issue Date: 2016-09-22

CHAPTER 5

Bordetella pertussis outer membrane vesicle vaccine confers equal efficacy in mice with a lower inflammatory response compared to a classic whole-cell vaccine

René H. M. Raeven^{1,2}, Jolanda Brummelman³, Jeroen L. A. Pennings⁴, Larissa van der Maas¹, Wichard Tilstra¹, Kina Helm³, Elly van Riet¹, Wim Jiskoot², Cécile A. C. M. van Els³, Wanda G. H. Han³, Gideon F. A. Kersten^{1,2}, Bernard Metz¹

¹Institute for Translational Vaccinology (Intravacc), Bilthoven, The Netherlands,

²Division of Drug Delivery Technology, Leiden Academic Centre for Drug Research, Leiden, The Netherlands,

³Centre for Infectious Disease Control, National Institute for Public Health and the Environment (RIVM), Bilthoven, The Netherlands,

⁴Centre for Health Protection (GZB), National Institute for Public Health and the Environment (RIVM), Bilthoven, The Netherlands

Submitted for publication

Abstract

Resurgence of whooping cough demands better understanding of the mode of action of pertussis vaccines. A systems biology approach was applied to investigate the immunogenicity, potency, and potential adverse effects in mice of a candidate outer membrane vesicles pertussis vaccine (omvPV) and a whole-cell pertussis vaccine (wPV) as comparator. To this end, responses were compared after (i) subcutaneous immunization and (ii) an intranasal *Bordetella pertussis* challenge. Both vaccines stimulated a mixed systemic response of Th1/Th2/Th17 cells. Remarkably, omvPV, as compared to wPV, evoked higher serum IgG levels, lower systemic pro-inflammatory cytokine responses, higher numbers of splenic neutrophils, and enhanced gene expression in the spleen. The transcriptome comprised gene signatures of the IFN-signaling pathway, anti-inflammatory signatures that attenuate LPS responses, anti-inflammatory metabolic signatures, IgG responses, and confirmed the presence of neutrophils. Upon intranasal challenge, mice immunized with omvPV or wPV were equally efficient in clearing *B. pertussis* from the lungs. Both immunized groups evoked diminished pulmonary and splenic gene transcription and pulmonary cytokine secretion as compared to challenged non-immunized mice. In conclusion, omvPV and wPV provide equal protection to bacterial colonization and induce a similar mixed Th1/Th2/Th17 response, while omvPV induced higher IgG levels. Moreover, omvPV elicited less pro-inflammatory cytokines, but more anti-inflammatory signatures. Therefore, milder inflammatory responses are observed in mice upon immunization with omvPV compared to wPV. These results emphasize the potential of omvPV as a third-generation pertussis vaccine.

Introduction

The efficacy of the pertussis vaccines on the market, whole-cell pertussis vaccine (wPV) and acellular pertussis vaccine (aPV), is under scrutiny because of the resurgence of whooping cough, despite high vaccination coverage [1, 2]. The current view on immunity to *B. pertussis* is that T-helper 1 and T-helper 17 (Th1/Th17) responses [3, 4] and specific antibody responses are preferred for protection. wPV induce a predominant Th1/Th17 response [4-6] and a broad systemic antibody repertoire [7], but wPV is associated with mild adverse effects [8, 9]. The suspected correlation between wPV and serious acute neurological illness in children [10, 11] has finally led to the call for safer pertussis vaccines. This resulted in the introduction of better-defined aPVs in many countries. The aPVs evoke high IgG1 antibody titers and mainly a Th2 response, which provides protection against disease, however, with a relatively short duration. Recent findings for aPV suggest waning immunity in children [12] and impaired prevention of transmission in baboons [13]. It is thought that the breadth of the antibody response [7] and the type of T-cell response induced by aPVs are suboptimal [14]. This situation calls for improved pertussis vaccines.

Outer membrane vesicles from *B. pertussis* are a potential vaccine candidate (omvPV). The protection in mice induced by omvPV is comparable to that of aPV, based on lung colonization data after *B. pertussis* challenge [15, 16]. Nevertheless, the omvPV elicits a broader humoral immunity compared to aPV [7]. To match the high short-term efficacy and good safety profile of current aPVs, a more comprehensive insight into omvPV-induced responses is required to unravel the type of immunity and assist in future vaccine registration. For this, an unbiased and detailed systems biology approach may be suitable. The application of systems biology in vaccine research has provided a better understanding of immune mechanisms and has been useful for the prediction of vaccine efficacy based on correlating biomarkers both for yellow fever and influenza [17-19]. Moreover, systems biology can be applied for comparing molecular signatures induced by distinct vaccines [20, 21] and for gaining insight into vaccine safety [22]. Previously we used a systems approach in mice to study *B. pertussis* infection-induced responses [23].

Here, a systems vaccinology approach is implemented to investigate the potency of omvPV in mice. In addition, wPV is included in the study as a benchmark. Furthermore, markers for vaccine safety are measured with respect to pro- and anti-inflammatory cytokine secretion and splenic transcriptome. Finally, immunized mice were subjected to a *B. pertussis* challenge to compare the induced immune responses to those in non-immunized mice.

Results

OmvPV provides slightly better protection than wPV against *B. pertussis* challenge

The composition of both omvPV and wPV, in terms of proteins, DNA, and LPS as well as particle size [7], was determined before mice were immunized twice with a four-week interval as illustrated in Figure 1. Vaccine efficacy was assessed by determining lung colonization in omvPV-immunized mice (omvPV-mice) compared to wPV- and non-immunized mice (wPV-mice and N.I.-mice, respectively) upon an intranasal challenge with *B. pertussis* (Figure 2A). As observed before [23], N.I.-mice showed extensive colonization and lungs were not cleared at day 77, the end of the observation time (21 days post challenge). The lungs of immunized mice were cleared faster. The lungs of omvPV-mice were cleared as fast as those of wPV-mice. Though omvPV-mice seemed to be even faster, no significant differences were found. In conclusion, this indicates that omvPV provides slightly better protection than wPV against *B. pertussis* challenge.

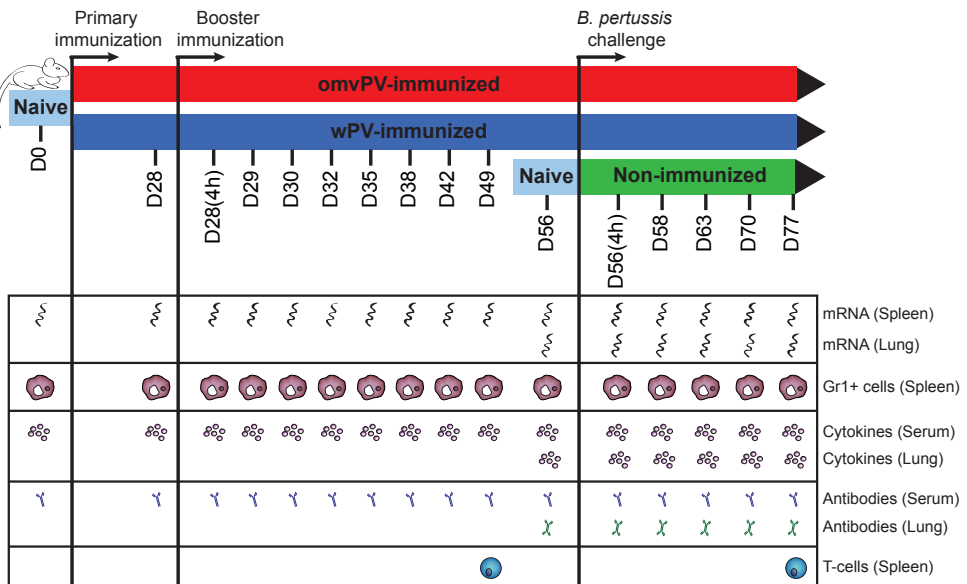


Figure 1 - Study design of the systems approach on omvPV- and wPV-induced responses. BALB/c mice were subcutaneously immunized with 4 µg omvPV (red) or wPV (blue) on day 0 and day 28. Subsequently, the vaccine-induced responses of both vaccines were characterized over a period of 56 days at 10 different time points. Additionally, an intranasal *B. pertussis* challenge (2×10^5 cfu/mouse) was performed on day 56 in immunized groups and in non-immunized mice (green). Both vaccine- and infection-induced responses were characterized at a transcriptomic, proteomic and cellular level on given time points, as depicted.

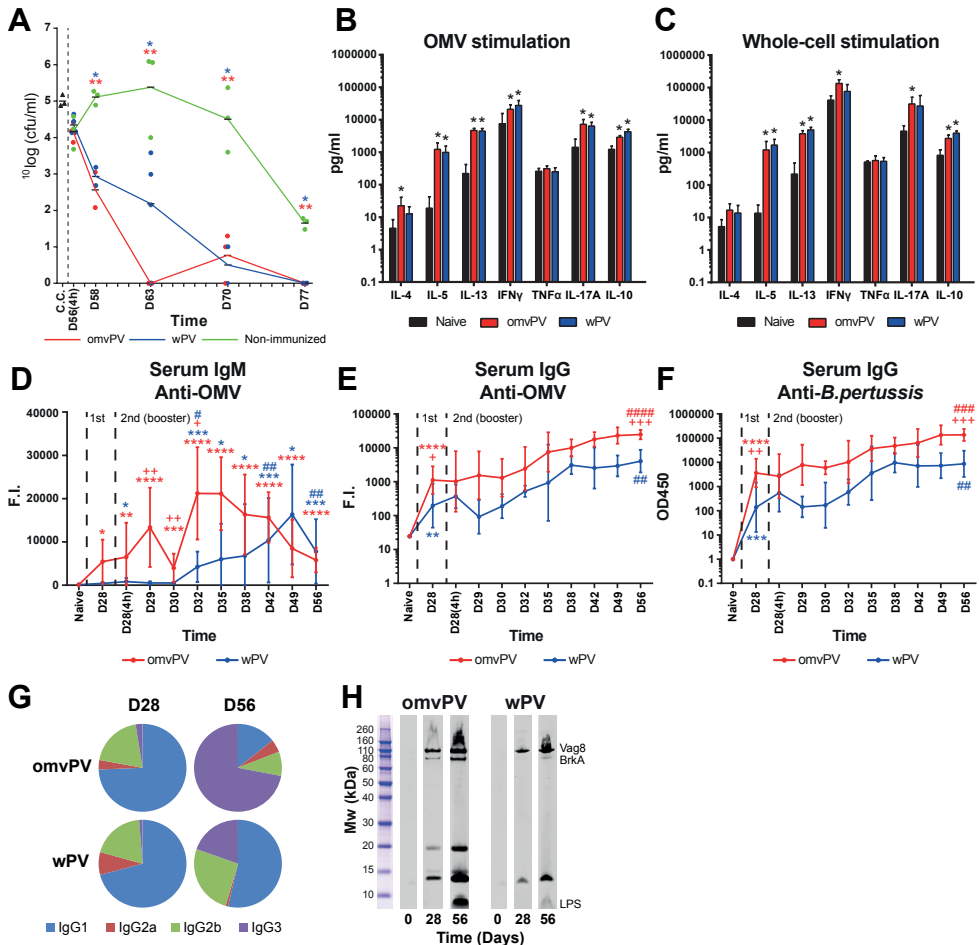


Figure 2 - Lung colonization and vaccine-induced adaptive responses in omvPV- and wPV-immunized mice. (A) Non-immunized, omvPV-immunized, and wPV-immunized mice were intranasally challenged with $2 \times 10^5/40 \mu\text{l}$ cfu *B. pertussis*. The number of cfu in 1 ml challenge culture (c.c.) was confirmed before challenge. Subsequently, the cfu/ml in the lungs of mice was determined 4 hours and 2, 7, 14, and 21 days after challenge (day 56(4h)-77). * and ** = $p \leq 0.05$ and $p \leq 0.01$ for immunized group vs. non-immunized group. (B-C) Splenocytes were obtained post booster immunization (day 49) of mice that were naive (black), omvPV-immunized (red), or wPV-immunized (blue). Concentrations of IL-4, IL-5, IL-13, IFN γ , TNF α , IL-17A and IL-10 were determined in the culture supernatants after 7 days of stimulation with (B) $5 \mu\text{g/ml}$ OMVs or (C) $5 \mu\text{g/ml}$ *B. pertussis* whole-cells. The results for each mouse are corrected for medium stimulation. Data presented as mean \pm SD ($n = 4$). * = $p \leq 0.05$ for immunized group vs. naive group. (D-H) The kinetics of serum (D) anti-OMV IgM, (E) anti-OMV IgG and (F) anti-*B. pertussis* IgG formation was determined for a period of 56 days after omvPV and wPV immunization. Data are presented as mean \pm SD ($n = 4$). For (D), *, **, *** and **** = $p \leq 0.05$, $p \leq 0.01$, $p \leq 0.001$ and $p \leq 0.0001$ for day 28-56 vs. naive, # and ## = $p \leq 0.05$ and $p \leq 0.01$, for day 28(4h)-56 vs. day 28, + and ++ = $p \leq 0.05$ and $p \leq 0.01$ for omvPV-mice vs. wPV-mice. For (E-F), *, **, *** and **** = $p \leq 0.05$, $p \leq 0.01$, $p \leq 0.001$ and $p \leq 0.0001$ for naive vs. day 28, #, ##, ### and #### = $p \leq 0.05$, $p \leq 0.01$, $p \leq 0.001$ and $p \leq 0.0001$ for day 28 vs. day 56, + and ++ = $p \leq 0.05$ and $p \leq 0.01$ for omvPV-mice vs. wPV-mice. The significance in (E) and (F) between day 28(4h)-49 is not depicted. (G) Subclass distribution was determined at day 56 in serum of mice immunized with omvPV or wPV by calculating the ratio of the level for each subclass from the sum of the levels all subclasses. (H) To determine antigen-specificity, the immunoproteomic profiles of serum antibodies (pooled sera, $n = 4$) following primary immunization (day 28) and booster immunization (day 56) were obtained. The band positions of Vag8, BrkA and LPS antigens, identified previously [7], are indicated.

OmvPV and wPV induce a mixed Th1/Th2/Th17 response

To investigate the vaccine-induced systemic T-cell responses, the levels of seven cytokines related to Th-responses were determined in culture supernatants from stimulated splenocytes harvested three weeks after the second immunization (Figure 2B-C). Stimulation with *B. pertussis* OMVs or whole-cells resulted in enhanced production of Th1 (IFN γ), Th2 (IL-5 and IL-13), and Th17 (IL-17A) cytokines and IL-10 in omvPV-mice and wPV-mice, compared to naive mice. TNF α was not observed, while IL-4 (Th2) was only detected after OMV stimulation of splenocytes from omvPV-mice. Upon stimulation of splenocytes with purified antigens, pertussis toxin (Ptx), filamentous hemagglutinin (FHA), and pertactin (Prn), hardly any cytokines were produced, with the exception of IL-17A after FHA stimulation of splenocytes from wPV-mice and IL-5 after Prn stimulation of splenocytes from omvPV-mice (Figure S3A-C, left panels). In conclusion, the cytokine profiles indicate that immunization of mice with omvPV and wPV generated a mixed repertoire of Th1/Th2/Th17 cells.

OmvPV induces higher serum IgG antibody responses

The IgG and IgM levels in mouse sera were monitored for 56 days (Figure 2D-F). omvPV induced IgM specific for OMV proteins and reached highest IgM levels on day 32 (Figure 2D). wPV also stimulated IgM production specific for OMV proteins, but at a slower rate and with a maximum level on day 49 (Figure 2D). Moderate IgG levels were detected 28 days after the primary immunization with either omvPV or wPV, detected by both a multiplex immunoassay (MIA) against OMVs and a whole-cell ELISA (Figure 2E-F). Booster immunization resulted in a strong increase of IgG production, with omvPV-mice developing higher IgG levels than wPV-mice. No IgG or IgM antibodies were found directed against purified antigens (Ptx, FHA, Prn, and Fimbriae 2 and 3 (Fim2/3)) (data not shown). The subclass distribution and immunoproteomic profiles of serum IgG antibodies were compared for both vaccines on day 28 and 56 (Figure 2G-H). The subclass distribution on day 28 was dominated by IgG1 for both omvPV and wPV (Figure 2G). However, booster immunizations with wPV and to a much larger extent with omvPV, stimulated production of IgG3 antibodies on day 56 (Figure 2G). As described previously, most of the IgG3 antibodies induced by omvPV and wPV immunization were shown to be specific for LPS [7]. Confirmed here, higher levels of anti-LPS IgG antibodies were detected after omvPV immunization compared to wPV immunization (Figure 2H). Moreover, these anti-LPS IgG antibodies were observed solely on day 56, indicating that these antibodies were elicited by the booster immunization. Additionally, both vaccines mainly induced antibodies specific for Vag8 and BrkA (Figure 2H).

Less pro-inflammatory cytokine induction in serum by omvPV compared to wPV

A MIA was performed on mouse sera to measure the vaccine-induced cytokine responses elicited by immunization with omvPV or wPV (Figure 3). Cytokine levels were mainly affected 4 hours after booster immunization (day 28(4h)), when the concentrations of CXCL10, G-CSF,

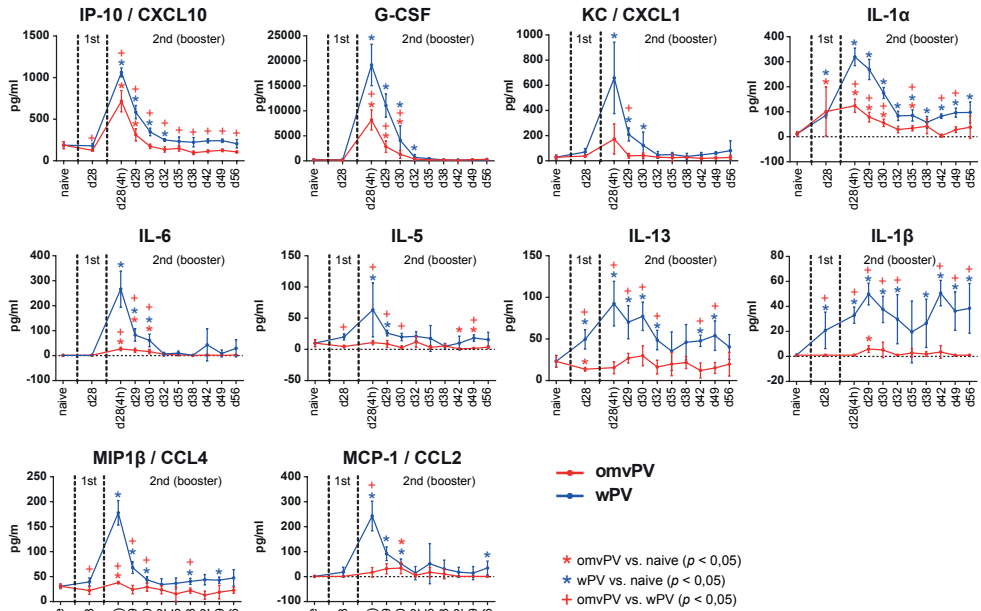


Figure 3 - Serum cytokine secretion following omvPV or wPV immunization. Concentrations of 32 cytokines were determined in serum at multiple time points after immunization with omvPV or wPV. Levels of CXCL10, G-CSF, CXCL1, IL-1 α , IL-6, IL-5, IL-13, IL-1 β , CCL4, and CCL2 were significantly altered and are depicted here. The different stages of primary immunization and booster immunization are depicted in the panels. Data represent mean \pm SD (n = 4). * = $p \leq 0.05$ for immunized group vs. naive, + = $p \leq 0.05$ for omvPV group vs. wPV group.

IL-1 α , IL-6 and CCL4 were significantly enhanced in omvPV-mice and wPV-mice compared to pre-immunization levels. In omvPV-mice, all these cytokine concentrations were significantly lower than in wPV-mice. Moreover, concentrations of CXCL1, CCL2, IL-1 β , IL-5, and IL-13 were only significantly elicited by the wPV booster immunization. These results indicate that the induction of pro-inflammatory cytokine levels is less intense after booster immunization with omvPV compared to wPV.

Transcriptomic profiles in the spleen induced by immunization with omvPV or wPV

Gene expression profiles were obtained in the spleen over a period of 28 days (day 28-56) to reveal the effects of immunization with omvPV or wPV. In total, 423 and 185 genes were identified that were differentially regulated compared to naive mice (day 0) (p -value ≤ 0.001 , Fold Ratio (FR) ≥ 1.5) in omvPV-mice and wPV-mice, respectively (Figure 4A). Of these genes, 160 (132 upregulated, 28 downregulated) overlapped between both immunized groups. Additionally, differential expression of 263 genes (180 upregulated, 83 downregulated) was exclusively detected in omvPV-mice, whereas 25 genes (21 upregulated, 4 downregulated) were only differentially regulated in wPV-mice (Figure 4A).

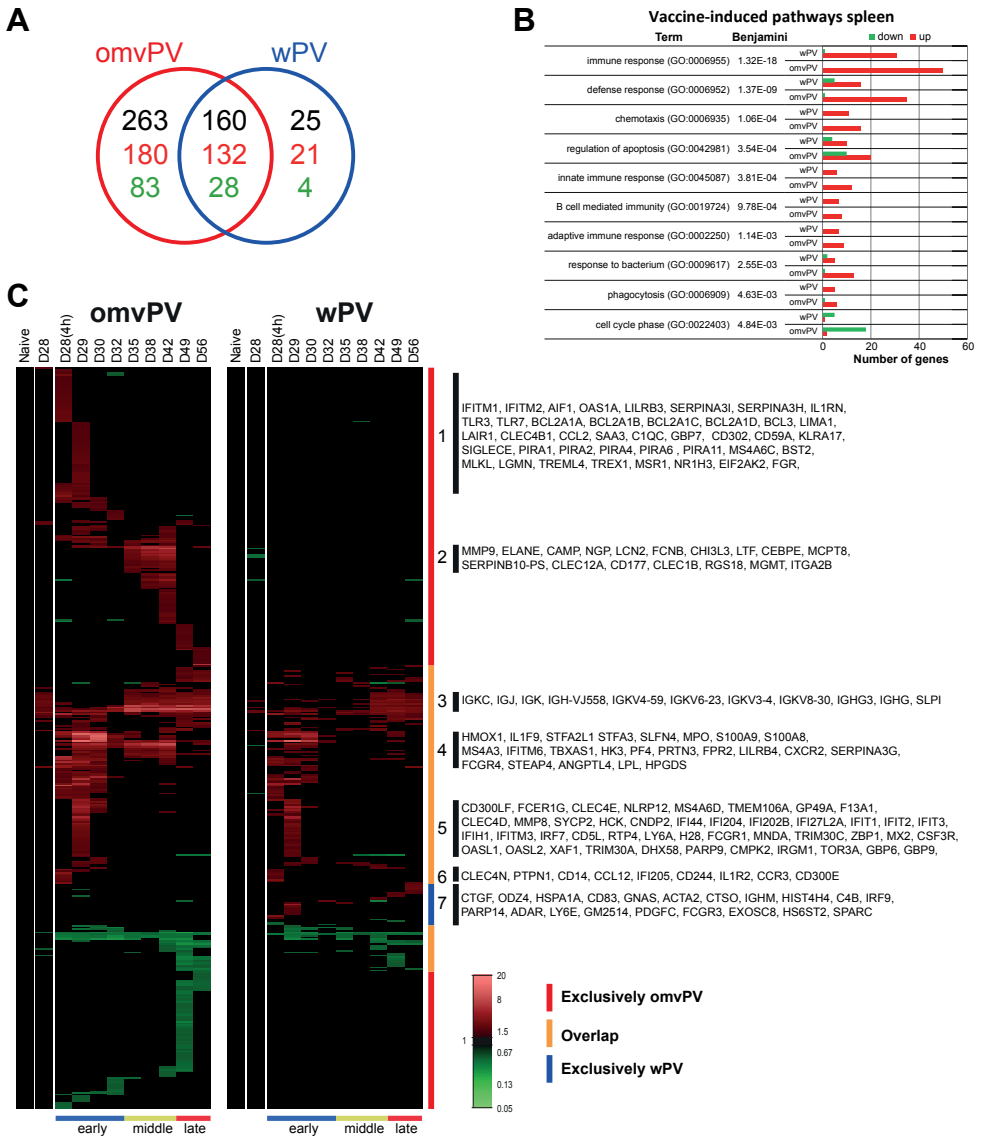


Figure 4 - Transcriptomic profiles in the spleen following omvPV and wPV booster immunization. (A) Fold changes of differentially expressed genes were calculated compared to naive mice ($FR \geq 1.5$, p -value ≤ 0.001). In total, 448 differentially expressed genes were found divided over both vaccine responses, as depicted in a Venn-diagram with total number of genes (black) and both upregulated (red) and downregulated genes (green). **(B)** Overrepresentation analysis on all 448 genes revealed the involvement of specific GO-BP terms and KEGG pathways with corresponding upregulated (red) and downregulated (green) genes. **(C)** All differentially upregulated (red) and downregulated (green) genes are portrayed as heatmap (mean of $n=4$). Genes not surpassing a FR of 1.5 are shown as basal level (black) at this time point. Gene clustering is based on up/downregulation, time of involvement, and presence in the immunization group. The overlap and the exclusive presence of differentially expressed genes in either the omvPV or wPV groups are further depicted next to the heatmap. Booster immunization-induced responses were divided in three phases: early phase (day 28(4h)-32), middle phase (day 35-42) and late phase (day 49-56) as calculated in [Figure S1A](#). Selections of genes co-expressed in seven (1-7) areas of the heatmap are shown.

To gain insight into the molecular pathways regulated by immunization, an overrepresentation analysis (ORA) was performed using DAVID. This analysis revealed enrichment of 77 gene ontology biological pathways (GO-BP) terms and 2 KEGG pathways (Benjamini ≤ 0.05) in the dataset of omvPV-mice and/or wPV-mice. The pathways related to immunity are shown in **Figure 4B**. The terms Immune response, Defense response, and Cell cycle contained more genes upregulated in omvPV-mice than in wPV-mice. Both groups have an equal number of genes related to Phagocytosis and B-cell mediated immunity (**Figure 4B**).

Genes were clustered based on (i) co-expression over time and (ii) overlap between both immunized groups (**Figure 4C**). Additionally, based on hierarchical clustering (**Figure S1A**), the time points in the vaccine-induced response could be divided in three phases; early phase (day 28(4h)-32), middle phase (day 35-42) and late phase (day 49-56) (**Figure 4C**). Based on the clustering of genes, 7 groups were identified that were further investigated in-depth using text mining and are described below.

Group 1 consists of genes that were detected exclusively in the early phase of the omvPV-induced response. This group comprised genes related to pathogen recognition, such as formyl peptide receptor 1 (*Fpr1*) and genes involved Toll-like receptor (TLR) 3 (*Tlr3*, *Mkl1*) and TLR7 (*Tlr7*, *Trem14*, *Lgmn*, *Trex1*) mediated signaling. *Trex1* limits the pro-inflammatory signals following TLR7 activation in macrophages [24], whereas *Siglec* represses TLR-signaling in general [25]. Moreover, members of the Bcl family, (*Bcl2a1a*, *Bcl2a1b*, *Bcl2a1c*, *Bcl2a1d*, *Bcl3*), paired-Ig-like receptors (*Pira1*, *Pira2*, *Pira4*, *Pira6*, *Pira11*, *Lilrb3*), IFN-induced transmembrane proteins 1 and 2 (*Ifitm1*, *Ifitm2*) and IL-1 receptor antagonist (*Il1rn*) were detected. In addition, enhanced expression was detected of the liver X receptor (*Nr1h3*), which is involved in lipid metabolism and an important mediator of inflammation in macrophages. Genes related to processing of LPS included *Bst2*, the macrophage scavenger receptor 1 (*Msr1*) that inhibits LPS-stimulated IL-6 secretion [26], and PKR (*Eif2ak2*), which is essential for LPS-induced iNOS production [27]. Finally, neutrophil-related genes (*Pram1*, *Fgr*), the C-type lectin receptor DCIR (*Clec4a2*), and two cytokines (*Ccl2*, *Saa3*) were found.

Group 2 genes were exclusively upregulated in the middle phase of the omvPV-induced response. This group contained genes related to myeloid cells (*Mcpt8*, *Clec12a*, *Chi3l3*) and more specifically neutrophil markers, including late stage neutrophil differentiation marker [28], lactotransferrin (*Ltf*), a neutrophil activation marker (*Clec1b*), *Cd177*, *Ngp*, and *Cebpe*. Moreover, the neutrophil-secreted lipocalin 2 (*Lcn2*), elastase (*Elane*), matrix metalloproteinase-9 (*Mmp9*), cathelicidin antimicrobial peptide (*Camp*), and ficolin B (*Fcnb*) were detected. Similar gene expression profiles were observed for *Rgs18*, *Mgmt*, and integrin alpha 2 (*Itgazb*).

Group 3 includes antibody-related genes, such as *Igkc*, *Igj*, *Igk*, and *Ighg*, which showed higher expression in omvPV-mice than in wPV-mice (**Figure 5A**), in line with the increased antibody levels (**Figure 2D-F**).

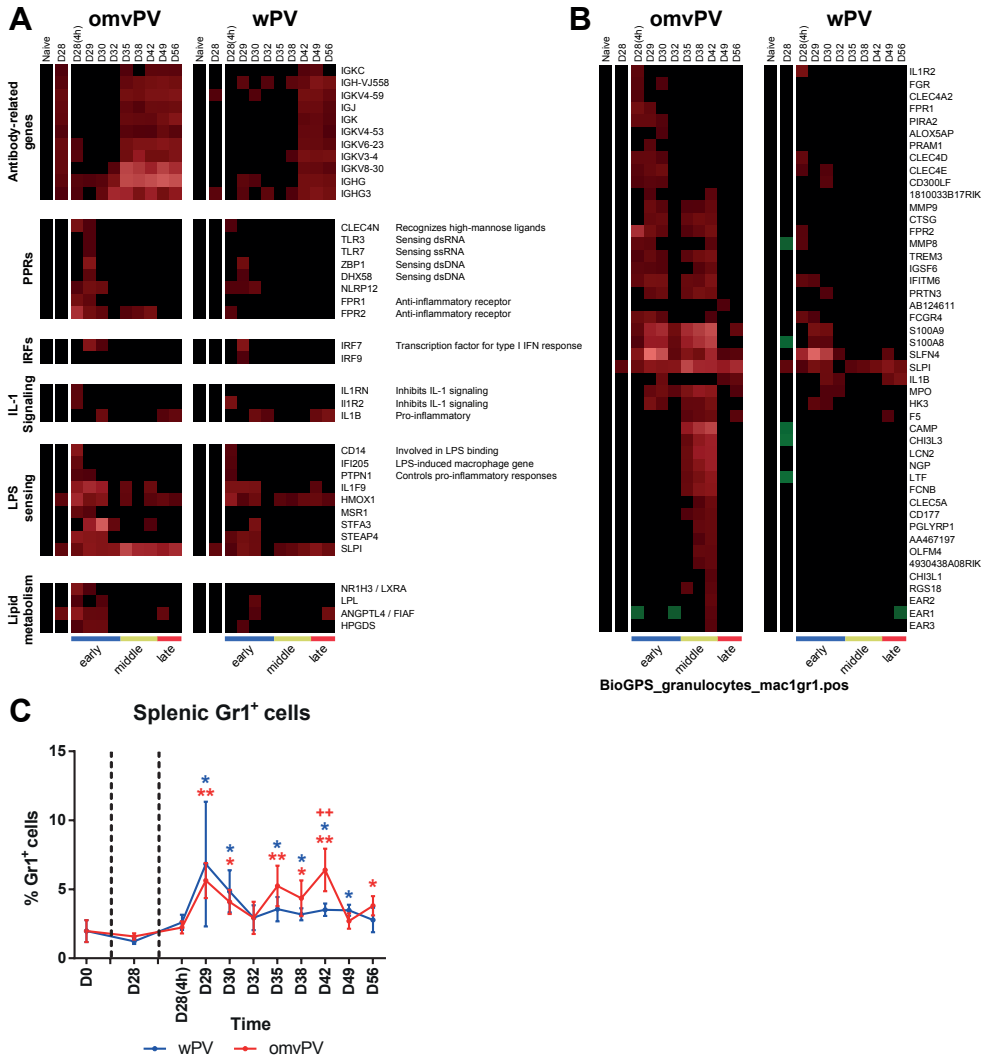


Figure 5 - Selected splenic transcriptome profiles and the involvement of Gr1⁺ cells following omvPV and wPV booster immunization. (A) The splenic transcriptome profiles of genes related to antibodies, pathogen recognition receptors (PRRs), interferon regulatory factors (IRFs), IL-1 signaling, LPS sensing, and lipid metabolism are depicted. (B) Transcriptomic profiles from spleen tissue of omvPV-mice and wPV-mice were compared with BioGPS databases. In total, 46 genes found following immunization showed overlap with the Mac1⁺Gr1⁺ granulocytes dataset, which are depicted as heatmap. (C) Flow cytometry was subsequently used to determine the percentage of Gr1⁺ cells in the spleen following omvPV and wPV immunization. Data presented as mean ± SD (n = 4). * and ** = p ≤ 0.05 and p < 0.01 for immunized mice vs. naive mice (day 0), ++ = p ≤ 0.01 for omvPV-mice vs. wPV-mice.

Group 4 genes were upregulated in the early phase of immunization in omvPV-mice, but were not or hardly upregulated in wPV-mice. In addition, most of these genes were differentially expressed in omvPV-mice during the middle phase, while the expression in wPV-mice was unaltered. This group contained the anti-inflammatory formyl-peptide receptor (*Fpr2*) [29]

and *Steap4* that decreases the inflammatory effect by repressing IL-6 production [30]. Moreover, genes involved in LPS responsiveness were upregulated, such as the secretory leukocyte peptidase inhibitor (*Sipi*) that suppresses responses to LPS [31], heme oxygenase 1 (*Hmox1*), *Stfa3* with a member of the same family *Stfa2l1*, and angiotensin-like 4 (*Angptl4*) that is induced by LPS in the acute phase response [32]. Notably, *Angptl4* has multiple functions, e.g. inflammation and lipid metabolism [33]. Genes involved in metabolism (*Hk3*, *Tbxas1*) and more specifically the lipid metabolism (*Angptl4*, *Lpl*, *Hpgds*) were found in this group. Furthermore, this group comprised *Pf4/Cxcl4* that induces phagocytosis [34], myeloid cell specific genes (*Lilrb4*, *Ms4a3*, *Serpina3g*), danger-associated molecular patterns (DAMPs) (*S100a9*, *S100a8*), IFN-induced genes *Slfn4* and *Ifitm6*, and *Fcgr4* that binds IgG2a and IgG2b. Moreover, genes were detected encoding proteins expressed on or secreted by neutrophils, such as myeloperoxidase (*Mpo*), proteinase 3 (*Prtn3*), a chemoattractant receptor (*Cxcr2*), and *Il1f9* [35]. IL-1F9 promotes Th1 formation by binding IL-36R on T-cells [36].

Group 5 genes were increased on day 29 by both vaccines. Some of these genes are involved in the type I IFN-signaling pathway. This included *Irf7* as well as *Oasl1* that inhibits IRF7 [37], in addition to other IFN-induced proteins (*Ifi44*, *Ifi204*, *Ifi202b*, *Ifi2712a*, *Ifit1*, *Ifit2*, *Ifit3*, *Ifih1*, *Ifitm3*, *Irgm1*, *H28*, *Mnda*, *Oasl2*, *Tor3a*, *Lgals3bp*, *Mx2*). Moreover, two genes were detected that encode PRRs which involved in sensing cytosolic DNA: DAI (*Zbp1*) [38] and LPG2 (*Dhx58*) [39]. Furthermore, genes encoding Fc receptors (*Fcgr1*, *Fcgr1g*), a NOD-like receptor (*Nlrp12*), which is a neutrophil migration marker [40], C-type lectins (*Clec4d*, *Clec4e*), and other membrane markers (*Ly6a*, *Ms4a6d*, *Cd300lf*, *Gp49a*) were identified. Moreover, differential gene expression was detected for matrix metalloproteinase-8 (*Mmp8*), hemopoietic cell kinase (*Hck*), LPS-induced gene (*Cmpk2*), the colony stimulating factor 3 receptor (*Csf3r*), genes involved in apoptosis (*Cd5l*, *Xaf1*), two members of the guanylate-binding protein gene family (*Gbp6*, *Gbp9*) that assist in protection against bacterial infection [41], and two genes encoding tripartite-motif proteins (*Trim30a*, *Trim30c*) of which TRIM30a inhibits TLR4-mediated NF-kappaB activation [42].

Group 6 genes were upregulated on day 28(4h) by both vaccines. This group included an LPS-induced macrophage gene (*Ifi205*), the inflammatory chemokine *Ccl12*, the interleukin 1 receptor, type II (*Il1r2*), and protein tyrosine phosphatase 1B (*Ptpn1*) that controls pro-inflammatory responses after LPS exposure [43]. Moreover, upregulated genes encoding membrane markers were detected that are mainly myeloid-restricted (*Cd300e*) of which some are related to pathogen-recognition, such as dectin-2 (*Clec4n*) that recognizes high-mannose ligands, *Cd14* commonly expressed on monocytes and involved in LPS binding, and other membrane markers (*Cd244*, *Ccr3*).

Group 7 genes were merely differentially expressed in the wPV-mice in the early phase after immunization. This group included increased gene expression of PDGFC (*Pdgfc*), IFN regulatory factor 9 (*Irf9*), complement component 4B (*C4b*), lymphocyte membrane marker (*Ly6e*), an Fc-receptor (*Fcgr3*), adenosine deaminase (*Adar*) that represses the effect after

bacterial DNA sensing, and PARP-14 (*Parp14*) that promotes Th2 and Th17 cell formation and steers the antibody subclass distribution [44, 45]. In the late phase after wPV immunization, ten genes were exclusively expressed including an IgM gene (*Ighm*), *Cd83* an important activation marker on B-cell, T-cell, and dendritic cell populations [46], and others (*Gnas*, *Ctso*, *Hspa1a*, *Acta2*, *Ctgf*, and *Odz4*).

Based on this text mining, sets of genes involved in antibody formation, pathogen recognition receptors (PRRs), interferon regulatory factors (IRFs), IL-1 signaling, LPS sensing and lipid metabolism were found (Figure 5A). For further investigation of genes related to IFN-signaling, the transcriptome of the spleen was matched with the Interferome database to identify which vaccine-induced genes were involved in the type I and type II IFN-signaling pathways (Figure S2). In total, 91 genes were related to type I IFN, 22 to type II IFN, and 60 genes to both pathways. The omvPV induced the majority of IFN-related genes of both type I and II, whereas only 13 of such genes were found exclusively in wPV-mice. Moreover, the type II IFN-signaling pathway was mainly involved in the early phase of the immune responses after omvPV and wPV immunization. Genes of the type I IFN-signaling pathway were also mainly found in the early phase, but also partly in later phases (Figure S2).

Together, comparison of the splenic transcriptomes after omvPV and wPV immunization demonstrated that omvPV conferred a more diverse and more intense gene expression compared to wPV. Moreover, omvPV activated genes are involved in pathogen-recognition, dampening of LPS-responses, IFN-related genes, lipid metabolism, neutrophils, and antibody production.

Higher neutrophil responses elicited by omvPV compared to wPV

Gene expression profiles were compared with BioGPS databases to identify which cell types were involved in vaccine-induced immune responses (Figure S1B). According to this analysis, 46 genes were associated with MAC⁺GR1⁺ granulocytes (neutrophils). All 46 genes were detected in omvPV-mice and were mainly activated during the early and middle phase of the vaccine-induced response (Figure 5B). In contrast, only 16 of these 46 genes were upregulated in the wPV-mice. Flow cytometry confirmed that the percentage of Gr1⁺ cells in the spleen was significantly increased by omvPV and wPV immunization between days 29-42 (Figure 5C). In line with the enhanced gene expression, the omvPV-induced response was characterized by a significant increase in Gr1⁺ cells in the middle phase on day 42 compared to the wPV-induced response.

Reduced serum and pulmonary cytokine responses in IMPV immunized mice following *B. pertussis* challenge

Subsequent to the investigation of vaccine-induced responses, we examined the immune responses in omvPV-mice, wPV-mice, and N.I.-mice after *B. pertussis* challenge by measuring gene expression profiles, cytokine profiles, splenic neutrophils, antibody levels, and T-cell responses (Figure 1).

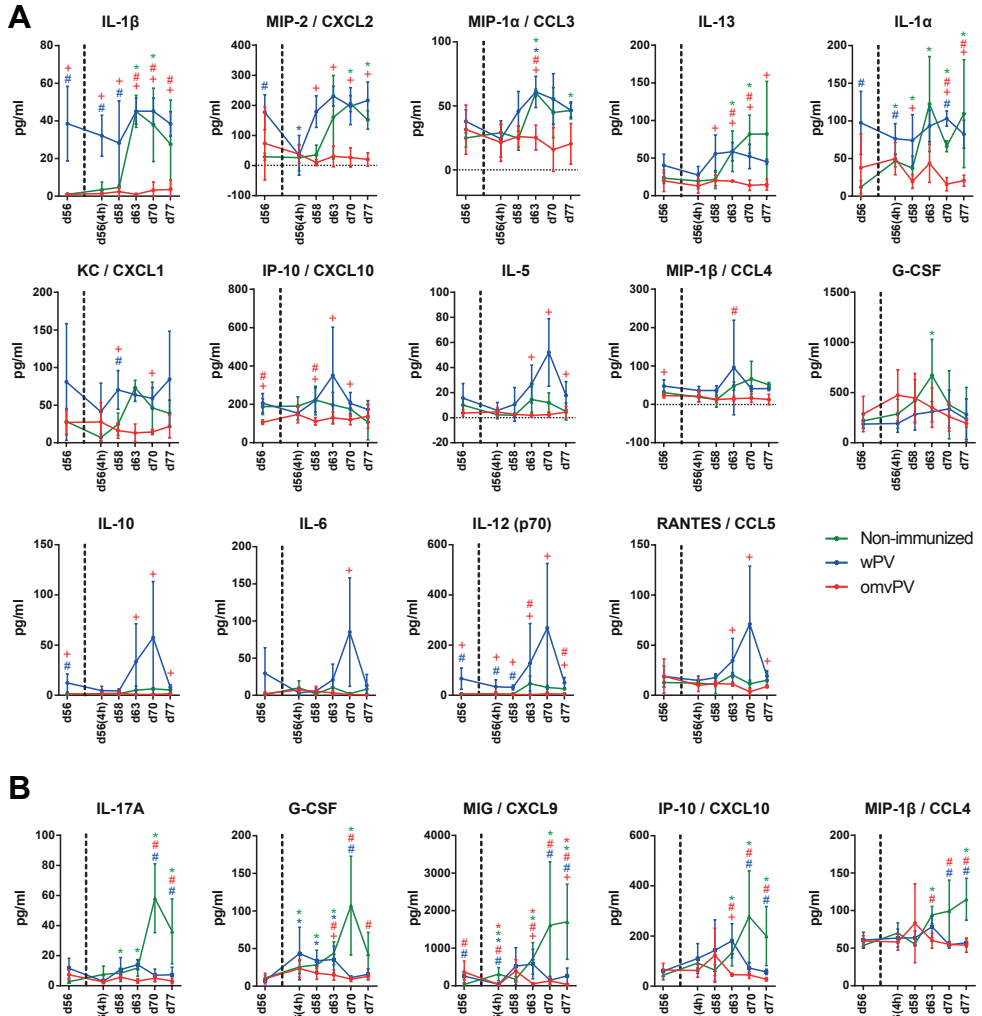


Figure 6 - Serum and pulmonary cytokine secretion following *B. pertussis* challenge in mice immunized with omvPV or wPV and non-immunized mice. (A-B) The concentrations of 32 cytokines were determined prior to and at multiple time points post challenge with *B. pertussis* in non-immunized mice (green) or mice immunized with omvPV (red) or wPV (blue). Only cytokines that were significantly altered in (A) serum and (B) lung lysate are depicted. Data are presented as mean \pm SD for immunized groups (n = 4) and non-immunized groups (n = 3). * = $p \leq 0.05$ for challenged groups vs. day 56, # = $p \leq 0.05$ for immunized groups vs. non-immunized group, + = $p \leq 0.05$ for omvPV group vs. wPV group.

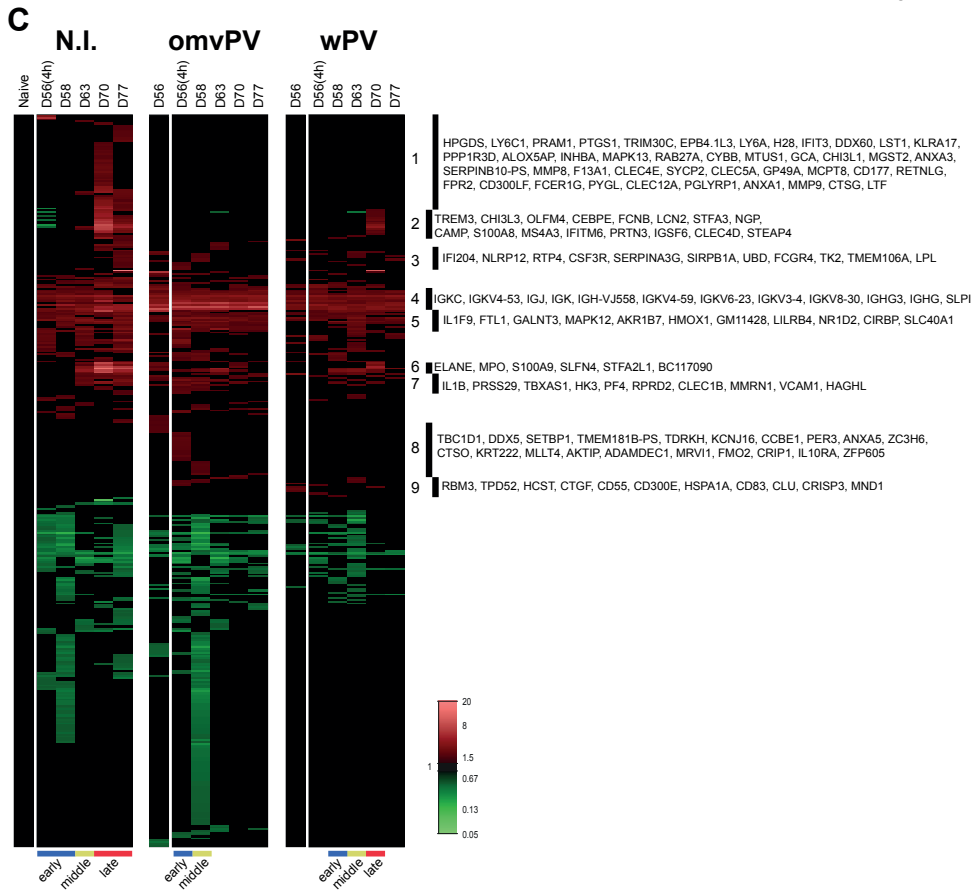
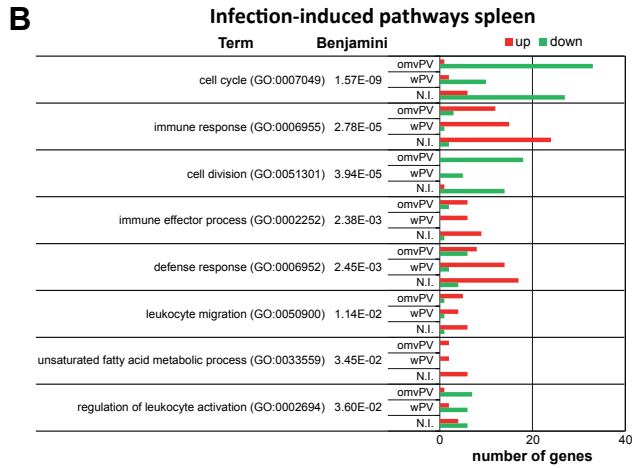
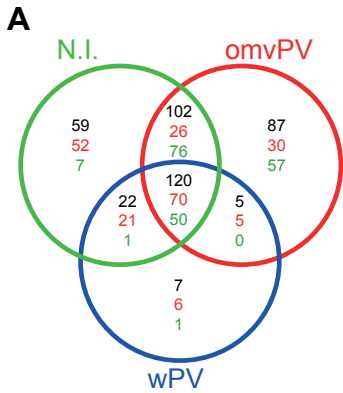


Figure 7 (Left) - Transcriptomic profiles in the spleen following *B. pertussis* challenge in omvPV-, wPV-, and non-immunized mice. (A) Fold changes in expression and significant gene expression were calculated compared to naive mice ($FR \geq 1.5$, $p\text{-value} \leq 0.001$). In total, 402 differentially expressed genes were found divided over the three groups in a Venn-diagram with total number of genes (black), upregulated genes (red), and downregulated genes (green). (B) Overrepresentation analysis on all 402 genes revealed the involvement of specific GO-BP terms and KEGG pathways with corresponding upregulated (red) and downregulated (green) genes. (C) All differentially upregulated (red) and downregulated (green) genes are portrayed as heatmap (mean of $n = 3$ for immunized groups, $n = 1$ (pool of 3 mice for non-immunized group)). Genes not surpassing a FR of 1.5 are shown as basal level (black). Gene clustering is based on up/downregulation, time of involvement, and presence in different groups. Infection-induced responses were divided in phases according to the hierarchical clustering calculated in [Figure S1C](#). Selections of genes in nine (1-9) areas of the heatmap are shown.

First, concentrations of 32 cytokines were determined in serum and lung lysate ([Figure 6A-B](#)). In sera of N.I.-mice, IL-1 α , IL-1 β , CXCL2, CCL3, IL-13, and G-CSF were significantly increased mainly between days 63-77. Notably, no significant cytokine secretion was observed in sera of omvPV-mice ([Figure 6A](#)). The concentrations of IL-1 α , IL-1 β , IL-5, IL-6, IL-10, IL-12(p70), IL-13, CCL3, CCL4, CCL5, CXCL1, CXCL2, and CXCL10 were significantly higher in the sera of wPV-mice compared to omvPV-mice, mainly on day 63. However, the cytokine levels of wPV-mice were not induced upon challenge, as no significant differences were found after challenge compared to day 56, except for CCL3 ([Figure 6A](#)). Analysis of the pulmonary cytokine profiles demonstrated that IL-17A, G-CSF, CXCL9, CCL4, and CXCL10 were significantly increased in lung tissue of N.I.-mice, between day 63-77 ([Figure 6B](#)). These cytokines were not elevated in either of the immunized groups, except for G-CSF in wPV-mice between day 56(4h)-63. These results demonstrate that both omvPV and wPV immunization prevented pulmonary cytokine secretion following a *B. pertussis* challenge. However, the systemic cytokine responses in wPV-mice appeared more like those in N.I.-mice, but different in omvPV-mice.

Transcriptomic profiles in the spleen following *B. pertussis* challenge

Splenic transcriptomes of immunized mice were compared to those of N.I.-mice at 5 timepoints after an intranasal challenge. In total, 402 genes were differentially expressed in the spleen of immunized mice or N.I.-mice ($p\text{-value} \leq 0.001$, $FR \geq 1.5$) ([Figure 7A](#)). Differential expression of 87, 7, and 59 genes was exclusively detected in the challenged omvPV-mice, wPV-mice, and N.I.-mice, respectively. 120 genes (70 upregulated, 50 downregulated) were found in all three groups ([Figure 7A](#)). The ORA on infection-induced responses in the spleen revealed enrichment of 24 gene ontology biological pathways (GO-BP) terms and 2 KEGG pathways (Benjamini ≤ 0.05) in omvPV-mice, wPV-mice, and N.I.-mice ([Figure 7B](#)). In omvPV-mice, several of the downregulated genes are involved in Cell cycle (33 genes) and Cell division (18 genes). The terms Immune response and Defense response comprised a small number of genes that were differentially regulated in omvPV-mice, but in higher numbers in wPV-mice and N.I.-mice. Genes were clustered based on (i) co-expression over time and (ii) overlap between both experimental groups ([Figure 7C](#)). Hierarchical clustering on the three challenged groups indicated that the infection-induced response was distinct in immunized mice compared to the

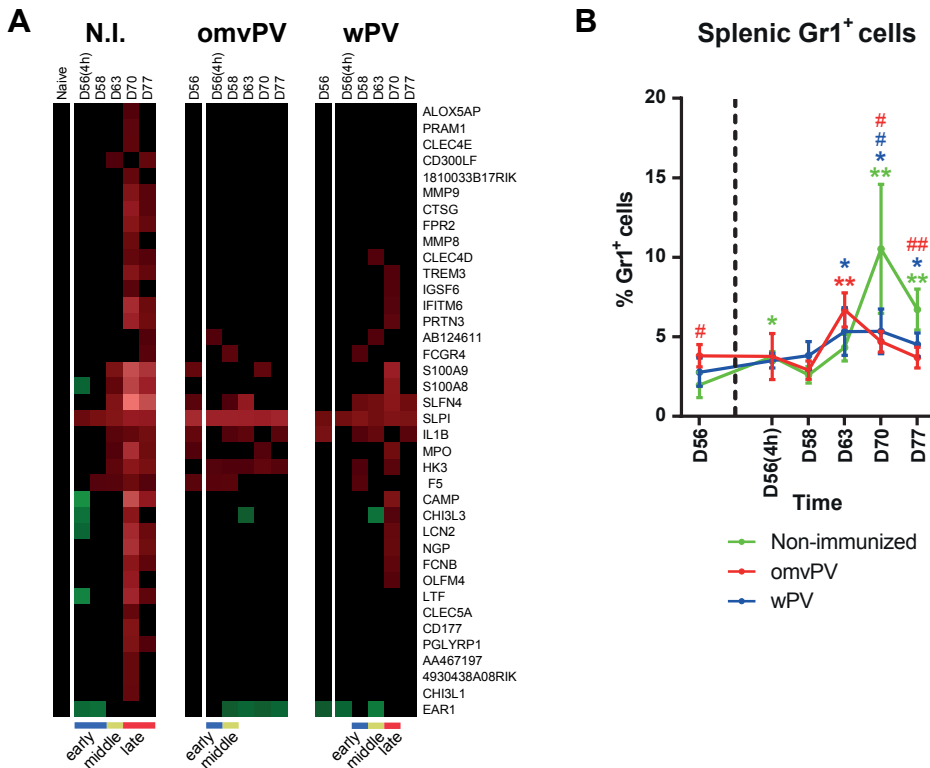


Figure 8 - Cell specific transcriptomic profiles and the involvement of Gr1⁺ cells after challenge of omvPV, wPV, and non-immunized mice. (A) Transcriptomic profiles from spleen tissue of omvPV-, wPV-, and non-immunized mice following a *B. pertussis* challenge were compared with BioGPS databases. In total, 38 differentially regulated genes matched with the Mac⁺Gr1⁺ granulocytes dataset and are depicted as heatmap. (B) Flow cytometry was used to determine the percentage of Gr1⁺ cells in the spleen after challenge of immunized and non-immunized mice. Data are presented as mean \pm SD ($n = 3$). * and ** = $p \leq 0.05$ and $p \leq 0.01$ for challenged groups vs. day 56, # and ## = $p \leq 0.05$ and $p \leq 0.01$ for immunized groups vs. non-immunized group.

challenged N.I.-mice (Figure S1C). The infection-induced response of N.I.-mice was divided in three phases: early phase (day 56(4h)-58), middle phase (day 63), and late phase (day 70-77). In omvPV-mice, a faster response was observed compared to N.I.-mice and was divided in two phases: early phase (day 56(4h)) and middle phase (day 58). The later time points (day 63-77) were similar to the expression levels prior to challenge (day 56). In wPV-mice, a slightly slower response compared to omvPV was seen and could be divided in an early phase (day 58), middle phase (day 63), and late phase (day 70) (Figure 7C and S1C). A selection of genes in nine (1-9) areas in the heatmap is depicted. BioGPS analysis revealed induction of 9 genes in challenged N.I.-mice that are usually expressed in MAC⁺GR1⁺ granulocytes (Figure 8A). In immunized mice, neutrophil involvement after challenge was much less pronounced as only 10 and 22 genes were found in omvPV-mice and wPV-mice, respectively. Additional flow cytometry analysis on splenocytes revealed that the number of Gr1⁺ cells, indicative for

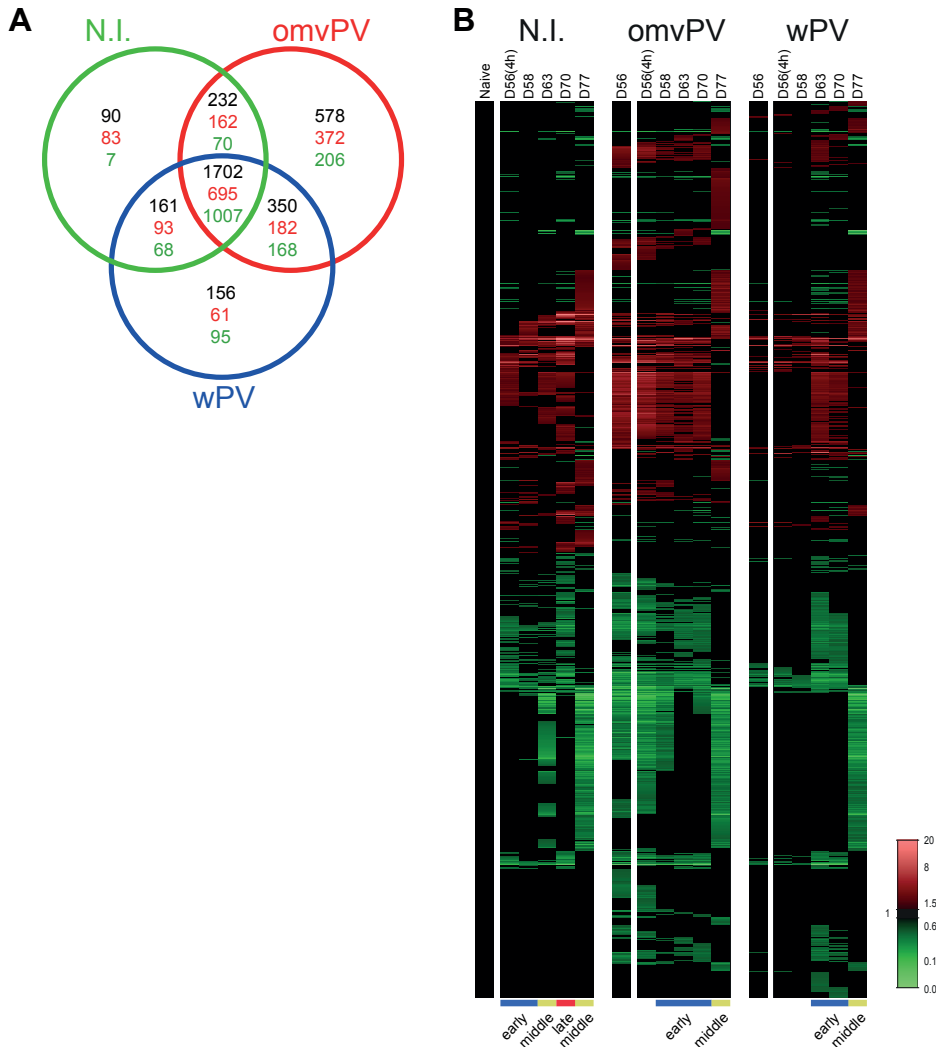


Figure 9 - Pulmonary transcriptomic profiles following *B. pertussis* challenge in omvPV- and wPV- and non-immunized mice. (A) Fold changes in expression and significant gene expression were calculated compared to naive mice ($FR \geq 1.5$, p -value ≤ 0.001). In total, 3269 differentially expressed genes were found divided over the three groups in a Venn-diagram with total number of genes (black), upregulated genes (red), and downregulated genes (green). (B) All differentially upregulated (red) and downregulated (green) genes are portrayed as heatmap (mean of $n = 3$ for immunized groups, $n = 1$ (pool of 3 mice for non-immunized group)). Genes not surpassing a FR of 1.5 are shown as basal level (black). Gene clustering is based on up/downregulation, time of involvement, and presence in the different groups. Infection-induced responses were divided in phases according to the hierarchical clustering calculated in [Figure S1D](#).

neutrophils, was significantly increased in N.I.-mice on day 70 ([Figure 8B](#)). In contrast, the fraction of $Gr1^+$ cells in omvPV-mice and wPV-mice was enhanced on day 63 and day 63-77, respectively. The $Gr1^+$ cell fraction in immunized mice was significantly lower between days 70-77 compared to N.I.-mice. Altogether, splenic transcriptome analysis after a challenge with

B. pertussis demonstrated less intense gene expression profiles in omvPV-mice and wPV-mice than in N.I.-mice. These responses were even lower in omvPV-mice than in wPV-mice.

Pulmonary transcriptomic profiles following *B. pertussis* challenge

To determine the effect of immunization on the murine host response in the lung following *B. pertussis* challenge, pulmonary transcriptomic profiles of challenged immunized mice were compared to those of challenged N.I.-mice. In total, 3269 genes were differentially expressed in lungs of immunized mice or N.I.-mice (p -value ≤ 0.001 , FR ≥ 1.5) (Figure 9A). Exclusive differential expression of 578, 156, and 90 genes was detected in challenged omvPV-mice, wPV-mice, and N.I.-mice, respectively. In total, 1702 genes (695 upregulated, 1007 downregulated) were found in all three groups (Figure 9A). Genes were clustered based on (i) co-expression over time and (ii) overlap between both experimental groups (Figure 9B). Hierarchical clustering on the pulmonary transcriptome of the three challenged groups demonstrated a distinct infection-induced response in immunized mice compared to challenged N.I.-mice (Figure S1D). The infection-induced response of N.I.-mice was divided in three phases: early phase (day 56(4h)-58), middle phase (day 63 and day 77) and late phase (day 70), as seen before [23]. In omvPV-mice, the response was less diverse compared to day 56 and was divided in two phases; early phase (day 56(4h)) and middle phase (day 70). In wPV-mice, the response compared to day 56 was more diverse and developed slower than in omvPV-mice with an early phase (day 63-70) and middle phase (day 77) (Figure 9B and S1D). The pulmonary transcriptome in omvPV-mice on day 56 prior to challenge differs a lot from the naive basal gene expression level. Moreover, omvPV-mice show less change in pulmonary gene expression as compared to wPV-mice and N.I.-mice after challenge. Together, these results demonstrate that a *B. pertussis* challenge evokes fewer effects on gene expression levels in omvPV-mice than wPV-mice and N.I.-mice.

Adaptive recall responses in omvPV-mice and wPV-mice following *B. pertussis* challenge

Prior to the challenge (day 56), no vaccine-induced anti-OMV IgA could be detected in the lungs of omvPV-mice and wPV-mice (Figure 10A). However, after intranasal *B. pertussis* challenge, anti-OMV IgA antibodies were detected in a similar amount in wPV-mice and N.I.-mice on day 63-77, yet not in omvPV-mice. Serum IgG levels specific for pertussis OMV or whole-cells were unaltered in wPV-mice and were slightly decreased in omvPV-mice after the intranasal challenge, whereas IgG levels in N.I.-mice were rising between day 63-77 (Figure 10B-C). The specificity of IgG antibodies, as determined by immunoblot, did not change in omvPV-mice after a challenge, except for the disappearance of the band at 15 kDa (Figure 10D). The challenge of wPV-mice led to the formation of additional antibodies directed against GroEL (60 kDa) and an unknown antigen of 20 kDa.

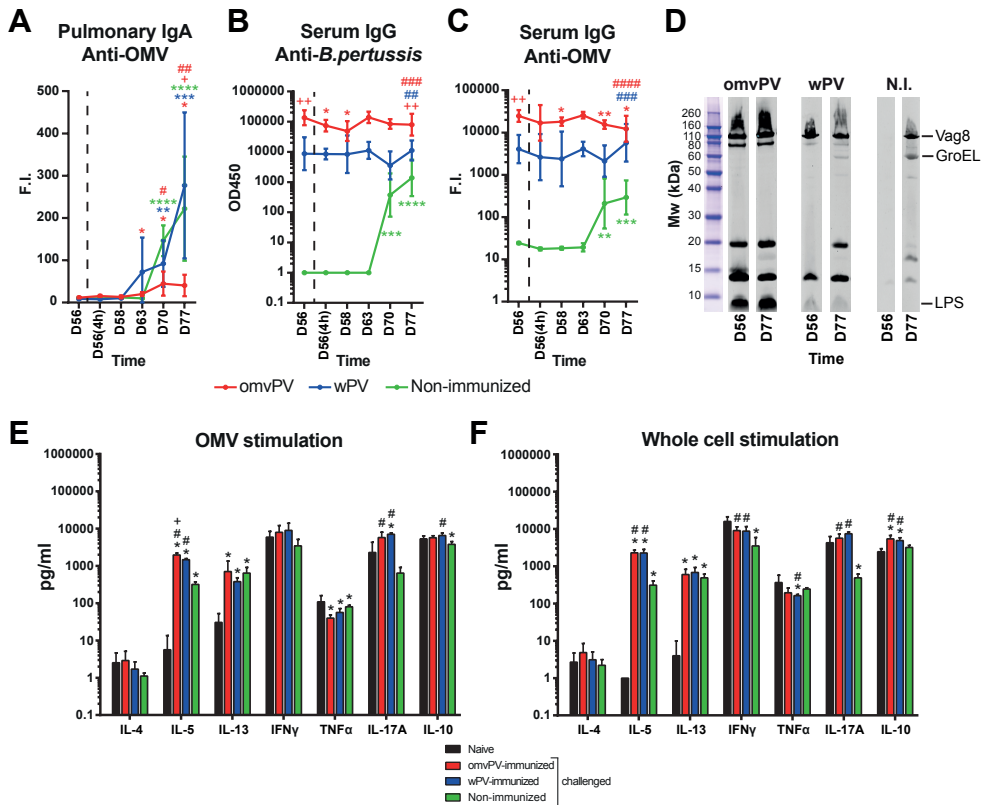


Figure 10 - Humoral and cellular adaptive recall responses following *B. pertussis* challenge in omvPV- and wPV-immunized mice as compared to control mice before and after challenge. (A-C) Kinetics of (A) pulmonary anti-OMV IgA, (B) serum anti-*B. pertussis* IgG, and (C) serum anti-OMV IgG levels were determined for a period of 21 days following intranasal challenge in immunized mice ($n = 4$) and non-immunized mice (N.I.) ($n = 3$). Data are presented as mean \pm SD. Statistical significance of differences in (A), (B) and (C): *, **, *** and **** = $p \leq 0.05$, $p \leq 0.01$, $p \leq 0.001$ and $p \leq 0.0001$ for vs. day 56 per group, + and ++ = $p \leq 0.05$ and $p \leq 0.01$ for omvPV vs. wPV, #, ##, ### and #### = $p \leq 0.05$, $p \leq 0.01$, $p \leq 0.001$ and $p \leq 0.0001$ for immunized groups vs. non-immunized group. (D) Immunoproteomic profiles of serum IgG antibodies (pooled sera, $n = 4$) before (day 56) and 21 days post challenge (day 77) were obtained on a *B. pertussis* lysate. (E-F) Concentrations of IL-4, IL-5, IL-13, IFN γ , TNF α , IL-17A and IL-10 were determined in the culture supernatants after 7 day stimulation with (E) 5 μ g/ml OMVs, or (F) 5 μ g/ml *B. pertussis* whole-cells. Splenocytes were obtained from naive mice (black) and post-challenge (day 77) of mice that were omvPV- (red), wPV- (blue) or non-immunized (green). Results for each mouse are corrected for medium stimulation. Data in (E) and (F) presented as mean \pm SD ($n = 4$). Statistical significance of differences in (E) and (F): * = $p \leq 0.05$ for challenged groups vs. naive, + = $p \leq 0.05$ for omvPV group vs. wPV group, # = $p \leq 0.05$ for immunized group vs. non-immunized group.

Th-responses were determined post challenge, by analyzing the levels of seven cytokines in culture supernatants after antigen-specific stimulation of splenocytes from challenged omvPV-mice, wPV-mice, and N.I.-mice, with those of non-challenged naive mice as control, harvested on day 77 (Figure 10E-F and S3). After stimulation with OMVs, Th1 (TNF α), Th2 (IL-5 and IL-13), and Th17 (IL-17A) cytokines were altered in challenged omvPV-mice, wPV-mice, and N.I.-mice compared to naive mice. IL-5 and IL-17A levels were higher in immunized mice compared to N.I.-mice (Figure 10E). Stimulation with *B. pertussis* whole-cells led to altered levels of Th1

(IFN γ), Th2 (IL-5 and IL-13) and Th17 (IL-17A) cytokines in omvPV-mice, wPV-mice, and N.I.-mice compared to naive mice. The levels of these cytokines were overall higher in immunized mice compared to N.I.-mice. Moreover, production of IL-10 was only observed in immunized mice (**Figure 10F**). IFN γ and TNF α were both high in naive control mice after stimulation with *B. pertussis* OMVs and whole-cells, most likely caused by LPS. Nevertheless, omvPV-mice and wPV-mice showed a similar result post challenge on day 77 as after immunization on day 49. Stimulation with Prn resulted in increased concentrations of IL-13 and IL-17A in challenged immunized and N.I.-mice compared to the non-challenged naive group (**Figure S3A, right panel**). These IL-17A levels were significantly higher in both immunized groups compared to the N.I.-mice. Furthermore, significantly higher IL-5 production was observed in omvPV-mice and N.I.-mice than in wPV-mice. After Ptx stimulation, IL-17A production was exclusively observed in wPV-mice (**Figure S3B, right panel**). IL-5, IL-13 and IL-17A production was evoked by FHA stimulation in immunized and N.I.-mice. Moreover, enhancement of IFN γ , TNF α , and IL-10 was detected in wPV-mice (**Figure S3C, right panel**). In conclusion, the cytokine profiles showed enhanced Th1/Th2/Th17 *ex vivo* recall responses in challenged omvPV-mice and wPV-mice compared to challenged N.I.-mice.

Discussion

Introduction of an improved third generation pertussis vaccine requires in-depth knowledge on vaccine-induced responses in comparison to current pertussis vaccines especially in terms of efficacy and safety profile. To that end, we applied a systems biology approach to compare comprehensive immune responses in a murine model induced by an OMV-based pertussis vaccine (omvPV) or a classical whole-cell pertussis vaccine (wPV).

Parenteral injection of wPV has been related to adverse effects [8, 9] and suspected correlation with serious acute neurological illness in children [10, 11] mainly as a result of circulating pro-inflammatory cytokines such as IL-1 β , TNF α , and IL-6 [11, 47]. This has been a key reason for the development of aPVs that are safer and better defined. Our *in vivo* study demonstrated that omvPV in comparison to wPV, with an equal total protein dose, elicited reduced concentrations of serum pro-inflammatory cytokines (IL-1 α , IL-1 β , and IL-6), chemokines (CXCL1 and CXCL10), and G-CSF. Especially, the reduced IL-1 β secretion by omvPV may be beneficial given its involvement in the suspected acute neurological illness [11]. Activation of Toll-like receptors (TLRs) [48] by pathogen-associated molecular patterns (PAMPs), like lipopolysaccharide (LPS) and bacterial DNA, result in the secretion of these cytokines. Previously we showed that the omvPV contains less TLR activating LPS and DNA per amount protein than wPV [7]. An additional hypothesis might be that omvPV contains mostly membrane-associated LPS and less free LPS compared to wPV thus resulting in lower cytokine induction. Less pro-inflammatory cytokine production was also seen when LPS is adsorbed to alum [49], which demonstrates that free LPS might be more pyrogenic than bound LPS. On the other hand, LPS in omvPV seems more immunogenic than LPS in wPV (Figure 2H). The lower concentrations of LPS and DNA in omvPV may therefore lead to less activation of TLR4 and TLR9 and contribute to the attenuated pro-inflammatory cytokine response by omvPV compared to wPV.

The splenic transcriptome measured after booster omvPV and wPV immunization demonstrated that omvPV induced a larger number of genes than wPV. This was an unexpected observation in light of the attenuated pro-inflammatory cytokine signatures. The triggering of anti-inflammatory responses, diminished PRR responses, and expression of modifiers that dampen inflammatory LPS responses in omvPV-mice may explain why omvPV elicited low amounts of pro-inflammatory cytokines. OmvPVs activated genes encoding anti-inflammatory formyl peptide receptors FPR1 and FPR2. These PRRs bind many different signal peptides of bacteria [50] which are important for rapid neutrophil recruitment [51]. Furthermore, the response induced by omvPV may repress pro-inflammatory responses following LPS recognition due to enhanced gene expression of FPR2, SPLI, STEAP4, PTPN1, and MSR1, which correspond to proteins that are attenuators of LPS responses [26, 29-31, 43].

Finally, omvPV stimulated genes encoding proteins with a dual function in lipid metabolism and anti-inflammatory responses, namely ANGPTL4 [32, 33], HPGD2S [52], and LXRA. These metabolic signatures may have been activated by lipid mediators induced by omvPV and may subsequently contribute to the anti-inflammatory response that is less prominent in the wPV-induced response. Despite the lower content of genomic DNA in omvPV [7], two genes encoding PRRs sensing cytosolic DNA, DAI [38], and LPG2 [39], were upregulated by both vaccines. Interestingly, only omvPV immunization led to enhanced gene expression of TLR3 and TLR7, intracellular sensors for viral and bacterial nucleotides. Activation of TLRs leads to induction of IFN-signaling pathways. For instance, we found induction of transcription factor IRF7, a factor downstream of TLR7, by both vaccines. IRF7 is an important mediator of type I IFN-signaling [53]. Overall, a large number of genes of the type I IFN-signaling pathway were induced by omvPV and wPV, which were more profound in the omvPV response. Type I IFN-signaling can affect a broad range of immune mediators, including both innate and adaptive immune cells [54]. With respect to CD4 T-cells, the pathway is important for the regulation of Th1 and Th17 responses [55]. Additionally, both vaccines induced many genes involved in the type II IFN-signaling pathway. IFN γ is the only member of the type II IFN family, for which upregulation of associated genes was again more profound in the omvPV response. Therefore, induction of both types of IFN-signaling pathways by omvPV and wPV seems to contribute to Th1/Th17 responses that are thought to be important for protection [3, 4, 23]. TLR4 activation by LPS is one of the pathways that can direct the cellular responses towards Th1 and Th17 responses [5, 6]. Thus, it is important to evaluate whether the reduced TLR4-signaling by omvPV does not affect the ability of omvPV to induce *B. pertussis*-specific Th1 and Th17 responses. Cytokine profiles of stimulated splenocytes revealed that omvPV and wPV both induce mixed systemic Th1/Th2/Th17 responses, in contrast to the Th2-biased aPV-induced response [4, 14]. This indicates that despite lower LPS concentration and TLR4-signaling, the omvPV still induced a similar Th response as wPV. This may suggest that the LPS concentration in omvPV is sufficient for the induction of Th1/Th17 responses or that other signaling, such as TLR2 [56], promote Th17 responses.

The concentrations of aPV components (Prn, FHA, and Ptx) are low in the omvPV and wPV used in this study, except for FHA in wPV [7]. Therefore, it was not surprising that antibody and T-cell responses specific for these antigens were low following immunization with omvPV and wPV. However, high levels of antibodies against other *B. pertussis*-specific antigens were detected that were more strongly induced by omvPV when compared to wPV. Especially the booster immunization induced a strong antibody response that was mainly directed against BrkA, Vag8 and LPS, in line with our previous study [7]. This broad humoral response conferred by both omvPV and wPV might limit the risk of driving *B. pertussis* adaptation as a result of vaccine-induced selection pressure. As Prn-deficient *B. pertussis* strains are increasingly circulating, especially in aPV-immunized populations, it has been hypothesized that this might be the result of pathogen adaptation [57, 58]. Since omvPV contains more BrkA and Vag8 [7],

higher antibody levels were induced against these antigens. Remarkably, despite the lower LPS concentrations measured in omvPV, the omvPV booster immunization induced higher anti-LPS IgG₃ antibody levels than wPV. This indicates that the LPS in omvPV was processed in a different way by the immune system during the first immunization compared to booster immunization. Since anti-LPS IgG₃ antibodies are mostly produced in a T-cell independent manner [59], this may indicate that omvPV evokes a more efficient T-cell independent B-cell response than wPV. Furthermore, mucosal *B. pertussis*-specific IgA induction in the lungs was absent after immunization with omvPV and wPV, as expected. Mucosal IgA is produced after natural infection [23, 60] and contributes most likely to a faster lung clearance during *B. pertussis* challenge. Presumably, direct involvement of the respiratory tract through intranasal or pulmonary vaccine administration may result in more effective immunity.

Mice immunized with omvPV or wPV showed rapid clearance of *B. pertussis* from the lungs after challenge when compared to N.I.-mice. Whereas no significant differences were observed between both immunized groups, lungs of omvPV-mice tended to be cleared slightly faster perhaps because of the higher serum IgG levels. Previously, intraperitoneal immunization with alum-adjuvanted omvPV and wPV derived from a *B. pertussis* Tohama strain also demonstrated equal protection [15]. The *B. pertussis* challenge was utilized to elucidate the pre-existing immunity in omvPV-mice and wPV-mice. The immune responses of challenged immunized mice were characterized by (i) adaptive recall responses, (ii) a change in pulmonary environment by reduced cytokine secretion and transcriptome expression, (iii) altered systemic cytokine responses, and (iv) reduced splenic transcriptome expression in comparison to challenged N.I.-mice. The presence of high serum IgG levels and the strong recall of Th1/Th2/Th17 responses enabled a rapid clearance in both immunized groups. In contrast to the vaccine-induced responses, the responses after challenge of immunized and N.I.-mice were characterized by detectable Th cytokines after stimulation with purified proteins, which indicates significant specific T-cell activation as a result of prolonged exposure to these antigens after *B. pertussis* challenge [23]. Furthermore, immunized mice responded less vigorous on an infection with respect to the splenic and pulmonary transcriptome, pulmonary and serum cytokine responses, and number of splenic neutrophils. The N.I.-mice showed the largest changes in gene expression in the lungs 14 days after challenge, which is in line with our previous study [23]. These responses were overall lower in omvPV-mice than wPV-mice. Finally, no IL-17A was secreted after *ex vivo* Ptx stimulation of splenocytes, and no antigen-specific IgA was detected in the lungs of challenged omvPV-mice, while these were present in both wPV-mice and N.I.-mice. This Ptx exposure occurred during *B. pertussis* colonization, as Ptx is absent in both omvPV and wPV used in this study [7]. Since the responses after *B. pertussis* challenge of wPV-mice and N.I.-mice show more similarities compared to those of omvPV-mice, this may indicate that omvPV-mice controlled the *B. pertussis* challenge more effectively than wPV-mice.

In summary, we demonstrated that in comparison to wPV, omvPV confers equal protection with higher IgG levels and a comparable Th1/Th2/Th17 response. Additionally, the systems approach provided detailed insight into the molecular signatures of the vaccine as well as challenge-induced responses. The inflammatory responses elicited by omvPV were milder, as reflected by reduced levels of pro-inflammatory cytokines. Probably, inflammatory responses are attenuated by the enhanced anti-inflammatory responses, i.e. ANGPTL4, FPR2, PTPN1, SPLI, and STEAP4. Therefore, it is tempting to speculate that the decreased inflammatory responses induced by omvPV reflect a better safety profile. In conclusion, our collective findings emphasize the potential of omvPV as a third-generation pertussis vaccine.

Methods

Vaccines and challenge culture

OmvPV from *B. pertussis* B1917 were produced as previously described [61]. For production of wPV, *B. pertussis* B1917 was heat-inactivated (30 min, 56°C) in PBS. Both omvPV and wPV were diluted in PBS to a final concentration of 4 µg total protein per immunization dose (300 µl). Vaccine characterization included particle size, protein composition, and LPS and DNA content [7]. For the challenge culture, stock suspension of *B. pertussis* strain B1917 was diluted with Verweij medium (BBio, Bilthoven, The Netherlands) to a final concentration of 5×10^6 colony-forming units (cfu)/ml.

Animal experiment

An independent ethical committee of the Institute for Translational Vaccinology (Intravacc) approved the animal experiment with identifier 201200073. 8 week old female BALB/c mice (Harlan, The Netherlands) were subcutaneously immunized with 4 µg total protein in 300 µl of either omvPV or wPV on day 0 (left groin) and day 28 (right groin). Mice were challenged intranasally under anesthesia (isoflurane/oxygen), with 2×10^5 cfu of *B. pertussis* B1917 in 40 µl of Verweij medium on day 56. Non-immunized (N.I.) mice were used as a control.

For the determination of gene expression in spleen, cytokine responses and antibody responses, mice (n = 4) were sacrificed on day 28 after primary immunization. In addition, mice (n = 4) were euthanized after booster immunization on day 28 + 4 hours (day 28(4h)), and day 29, 30, 32, 35, 38, 42, 49 and 56. Finally, mice (n = 4 per group) were sacrificed 4 hours after challenge and on day 58, 63, 70, and 77 to measure bacterial load in the respiratory tract, antibody responses and cytokine responses. For the investigation of Th subsets, mice (n = 4) were sacrificed on day 49 and 84. Naive mice (n = 4) were included as additional control group on each time point. Mice were bled under anesthesia (isoflurane/oxygen) by orbital bleeding and sacrificed by cervical dislocation for further sample collection. An overview of the study design is depicted in [Figure 1A](#).

Sample collection and preparation

For investigation of cytokine and antibody responses in serum, whole blood from each mouse was collected in a blood collection tube (MiniCollect 0.8 ml Z Serum Sep GOLD, Greiner Bio-One, Austria). After coagulation (10 min. at room temperature) and centrifugation (10 min., 3000 g), sera were taken and stored at -80°C. For the colonization assay, the right lung lobe was placed in 900 ml Verweij medium at room temperature. To determine pulmonary cytokine and antibody responses, the lung lysates used for colonization assays were filtered (Millex GV Filter unit 0.22 µm, Millipore) and stored at -80°C. For characterization of pulmonary gene expression, the left lung lobe was placed in 1 ml RNeasy lysis buffer (Qiagen), incubated overnight at 4°C, and stored at -80°C. In addition, the spleen was excised and divided in two equal parts.

For gene expression analysis, one piece was placed in 1 ml RNAlater (Qiagen), incubated overnight at 4°C and stored at -80°C. For detection of Gr1⁺ cells, the other piece was placed in 5 ml RPMI-1640 medium (Gibco) supplemented with 10% FCS (Hyclone), 100 units penicillin, 100 units streptomycin, and 2.92 mg/ml L-glutamine (Invitrogen), hereafter called RPMI complete medium, and kept on ice. For the analysis of Th responses, the whole spleen was placed in 5 ml of RPMI medium and kept on ice. Splenocytes were isolated by homogenization of spleens using a 70- μ m cell strainer (BD Falcon, BD Biosciences) in RPMI complete medium.

Colonization assay

The numbers of cfu in lung tissue were determined as previously described [23].

RNA isolation and microarray analysis

Isolation and determination of concentration and integrity of RNA obtained from lung and spleen tissue were performed as described before [23]. For spleen tissue of both omvPV-mice and wPV-mice, individual RNA concentrates of individual mice ($n = 3$) were analyzed for all 16 time points (naive, and day 28, 28(4h), 29, 30, 31, 32, 35, 42, 49, 56, 56(4h), 58, 63, 70, and 77 post primary immunization). For lung tissue, samples of individual mice were analyzed for the following time points: day 56(4h), 58, 63, 70, and 77 post primary immunization. For the non-immunized mice after challenge, samples of lung and spleen tissue were pooled ($n = 3$). Amplification, labeling and hybridization of RNA samples for either lung or spleen tissue to microarray chips (NimbleGen 126135 k Mus musculus, Roche, Germany) was carried out at the Microarray Department of the University of Amsterdam, The Netherlands, as described previously [23].

Data analysis of gene expression

Quality control and normalization of raw microarray data was performed as described before [23]. To identify differentially expressed genes between experimental groups (naive and various time points post immunization or challenge) an ANOVA was applied. The induction or repression of individual genes was expressed as fold ratio (FR) by comparing mean gene expression levels of experimental groups to the naive mice. Average normalized gene expression levels contain data of three mice per immunized group. The data of challenged non-immunized mice are individual samples of pooled RNA of three mice. The dataset of challenged non-immunized mice ($n = 3$) of our previous study [23] was incorporated in the analysis to increase the statistical power. Probes were considered differentially expressed if they met the following two criteria: (i) a p -value < 0.001 (ANOVA), which corresponds to a Benjamini-Hochberg False discovery rate (FDR) [62] of $< 5\%$; and (ii) an absolute FR ≥ 1.5 (experimental groups compared to naive mice) for at least one time point. If multiple probes corresponding to the same gene were differentially expressed, their data were averaged to remove redundancy for further analysis. GeneMaths XT (Applied Maths, St-Martens-Latem,

Belgium) was used to visualize differences in gene expression in heatmaps and perform the hierarchical clustering using Euclidean distance (linear scaling) with UPGMA clustering. Genes were arranged according to similar expression patterns in time at which genes exceeded the FR cut-off of 1.5. To facilitate visual interpretation of heatmaps, only induction (red) and repression (green) of gene expression levels with fold ratios ≥ 1.5 are visualized, therefore presenting fold ratios ≤ 1.5 as naive level (black). Functional enrichment with an over-representation analysis (ORA) based on Gene Ontology Biological Processes (GO-BP) and Kyoto Encyclopedia of Genes and Genomes (KEGG) by using DAVID and the detection of cell-specific or tissue-specific gene expression based on BioGPS datasets was performed as described previously [23]. Involvement of type I and II IFN-signaling pathway was performed by using the Interferome database (<http://www.interferome.org/interferome/home.jspx>) [63]. Additional text mining on gene function was performed in PubMed.

Multiplex immunoassay (MIA) and ELISA for antibody response

Levels of pulmonary IgA and serum IgM, IgA, total IgG and IgG subclasses (IgG1, IgG2a, IgG2b and IgG3) specific for *B. pertussis* antigens Prn, FHA, Ptx, combined fimbria type 2 and 3 antigens (Fim2/3) and outer membrane vesicles B1917 (OMV B1917) were determined as described previously [23] and are presented as fluorescent intensity (F.I.). Whole-cell *B. pertussis* ELISA for total serum IgG was performed as described before [23].

Immunoproteomic profiling of serum IgG antibodies

Antigen specificity of *B. pertussis*-specific serum IgG antibody responses were determined by SDS-PAGE and subsequent Western blotting as described before [7].

Gr1⁺ cells in the spleen

After treatment with erythrocyte lysis buffer (8.3 g/L NH₄CL, 1 g/L NaHCO₃, 5000 IE/L Heparin in dH₂O; pH 7.4), the percentage of Gr1⁺ cells in the spleen was determined with flow cytometry as described before [23].

Isolation and *in vitro* restimulation of splenocytes

After treatment with erythrocyte lysis buffer, splenocytes were cultured in 24-well plates at 6×10^6 cells/well for 7 days at 37°C in a humidified atmosphere containing 5% CO₂ in IMDM medium (Gibco) supplemented with 8% FCS, 100 units penicillin, 100 units streptomycin, 2.92 mg/ml L-glutamine, and 20 μM β-mercaptoethanol (Sigma). The cells were either left unstimulated (medium control) or stimulated with 1 μg/ml, 1 μg/ml Ptx, 1 μg/ml FHA, 5 μg/ml OMV, or 5 μg/ml heat-killed *B. pertussis*. *B. pertussis* antigens Ptx and FHA were obtained from Kaketsuken (Japan), Prn and Fim2/3 were kindly provided by Betsy Kuipers (National Institute for Public Health and the Environment, Bilthoven, the Netherlands). On day 7, supernatant was collected for cytokine analysis.

Cytokine profiling using multiplex technology

Concentrations (pg/ml) of 32 cytokines (Eotaxin, G-CSF, GM-CSF, IFN γ , IL-10, IL-12 (p40), IL-12 (p70), IL-13, IL-15, IL-17A, IL-1 α , IL-1 β , IL-2, IL-3, IL-4, IL-5, IL-6, IL-7, IL-9, IP-10, KC, LIF, LIX, M-CSF, MCP-1, MIG, MIP-1 α , MIP-1 β , MIP-2, RANTES, TNF α , VEGF) present in serum and lung lysates were determined by using a MIA (Milliplex MAP Mouse Cytokine/ Chemokine - Premixed 32 Plex; Merck KGaA, Darmstadt, Germany) following the manufacturer's protocol.

The concentration of various Th cytokines (IL-4, IL-5, IL-10, IL-13, IL-17A, TNF α , and IFN γ) was determined in culture supernatant using a Milliplex mouse cytokine 7-plex luminex kit (Millipore), according to the manufacturer's protocol. Measurements and data analysis were performed with Bio-Plex 200, using Bio-PlexManager software (version 5.0, Bio-Rad Laboratories). Results were corrected for the background (medium control) per mouse per stimulation per cytokine and calculated in pg/ml.

Statistical analysis

Data of the antibody, cytokine, and colonization assays were log-transformed after which a t-test was performed. *P*-values ≤ 0.05 were considered to indicate significant differences.

Acknowledgments

The authors are grateful to Tim Bindels of Intravacc for the production of the omvPV. The authors thank employees of the Animal Research Centre (ARC) of Intravacc for the performance of animal experiments, and employees of the Microarray Department (MAD) of the University of Amsterdam for the performance of the microarray analyses.

References

- Cherry, J.D., Epidemic pertussis in 2012—the resurgence of a vaccine-preventable disease. *N Engl J Med*, 2012. 367(9): p. 785-7.
- Tan, T., et al., Pertussis Across the Globe: Recent Epidemiologic Trends From 2000-2013. *Pediatr Infect Dis J*, 2015. 34(9): p. e222-32.
- Warfel, J.M. and T.J. Merkel, *Bordetella pertussis* infection induces a mucosal IL-17 response and long-lived Th17 and Th1 immune memory cells in nonhuman primates. *Mucosal Immunol*, 2013. 6(4): p. 787-96.
- Ross, P.J., et al., Relative contribution of Th1 and Th17 cells in adaptive immunity to *Bordetella pertussis*: towards the rational design of an improved acellular pertussis vaccine. *PLoS Pathog*, 2013. 9(4): p. e1003264.
- Higgins, S.C., et al., TLR4 mediates vaccine-induced protective cellular immunity to *Bordetella pertussis*: role of IL-17-producing T cells. *J Immunol*, 2006. 177(11): p. 7980-9.
- Banus, S., et al., The role of Toll-like receptor-4 in pertussis vaccine-induced immunity. *BMC Immunol*, 2008. 9: p. 21.
- Raeven, R.H.M., et al., Immunoproteomic Profiling of *Bordetella pertussis* Outer Membrane Vesicle Vaccine Reveals Broad and Balanced Humoral Immunogenicity. *J Proteome Res*, 2015. 14(7): p. 2929-42.
- Jefferson, T., M. Rudin, and C. DiPietrantonj, Systematic review of the effects of pertussis vaccines in children. *Vaccine*, 2003. 21(17-18): p. 2003-14.
- David, S., P.E. Vermeer-de Bondt, and N.A. van der Maas, Reactogenicity of infant whole cell pertussis combination vaccine compared with acellular pertussis vaccines with or without simultaneous pneumococcal vaccine in the Netherlands. *Vaccine*, 2008. 26(46): p. 5883-7.
- Miller, D.L., et al., Pertussis immunisation and serious acute neurological illness in children. *Br Med J (Clin Res Ed)*, 1981. 282(6276): p. 1595-9.
- Armstrong, M.E., et al., IL-1beta-dependent neurological effects of the whole cell pertussis vaccine: a role for IL-1-associated signalling components in vaccine reactogenicity. *J Neuroimmunol*, 2003. 136(1-2): p. 25-33.
- Klein, N.P., et al., Waning protection after fifth dose of acellular pertussis vaccine in children. *N Engl J Med*, 2012. 367(11): p. 1012-9.
- Warfel, J.M., L.I. Zimmerman, and T.J. Merkel, Acellular pertussis vaccines protect against disease but fail to prevent infection and transmission in a nonhuman primate model. *Proc Natl Acad Sci U S A*, 2014. 111(2): p. 787-92.
- Brummelman, J., et al., Modulation of the CD4 T cell response after acellular pertussis vaccination in the presence of TLR4 ligation. *Vaccine*, 2015. 33(12): p. 1483-91.
- Roberts, R., et al., Outer membrane vesicles as acellular vaccine against pertussis. *Vaccine*, 2008. 26(36): p. 4639-46.
- Gaillard, M.E., et al., Acellular pertussis vaccine based on outer membrane vesicles capable of conferring both long-lasting immunity and protection against different strain genotypes. *Vaccine*, 2014. 32(8): p. 931-7.
- Nakaya, H.I., et al., Systems biology of vaccination for seasonal influenza in humans. *Nat Immunol*, 2011. 12(8): p. 786-95.
- Furman, D., et al., Apoptosis and other immune biomarkers predict influenza vaccine responsiveness. *Mol Syst Biol*, 2013. 9: p. 659.
- Querec, T.D., et al., Systems biology approach predicts immunogenicity of the yellow fever vaccine in humans. *Nat Immunol*, 2009. 10(1): p. 116-25.
- Obermoser, G., et al., Systems scale interactive exploration reveals quantitative and qualitative differences in response to influenza and pneumococcal vaccines. *Immunity*, 2013. 38(4): p. 831-44.
- Li, S., et al., Molecular signatures of antibody responses derived from a systems biology study of five human vaccines. *Nat Immunol*, 2014. 15(2): p. 195-204.
- Mizukami, T., et al., System vaccinology for the evaluation of influenza vaccine safety by multiplex gene detection of novel biomarkers in a preclinical study and batch release test. *PLoS One*, 2014. 9(7): p. e101835.
- Raeven, R.H.M., et al., Molecular Signatures of the Evolving Immune Response in Mice following a *Bordetella pertussis* Infection. *PLoS One*, 2014. 9(8): p. e104548.
- Pereira-Lopes, S., et al., The exonuclease Trex1 restrains macrophage proinflammatory activation. *J Immunol*, 2013. 191(12): p. 6128-35.
- Chen, G.Y., et al., Broad and direct interaction between TLR and Siglec families of pattern recognition receptors and its regulation by Neu1. *Elife*, 2014. 3: p. e04066.
- Jozefowski, S., et al., The class A scavenger receptor SR-A/CD204 and the class B scavenger receptor CD36 regulate immune functions of macrophages differently. *Innate Immun*, 2014. 20(8): p. 826-47.
- He, Y., L. Franchi, and G. Nunez, The protein kinase PKR is critical for LPS-induced iNOS production but dispensable for inflammasome activation in macrophages. *Eur J Immunol*, 2013. 43(5): p. 1147-52.
- Kovacic, B., et al., Lactotransferrin-Cre reporter mice trace neutrophils, monocytes/macrophages and distinct subtypes of dendritic cells. *Haematologica*, 2014. 99(6): p. 1006-15.
- Dufton, N., et al., Anti-inflammatory role of the murine formyl-peptide receptor 2: ligand-specific effects on leukocyte responses and experimental inflammation. *J Immunol*, 2010. 184(5): p. 2611-9.
- Inoue, A., et al., Murine tumor necrosis factor alpha-induced adipose-related protein (tumor necrosis factor alpha-induced protein 9) deficiency leads to arthritis via interleukin-6 overproduction with enhanced NF-kappaB, STAT-3 signaling, and dysregulated apoptosis of macrophages. *Arthritis Rheum*, 2012. 64(12): p. 3877-85.
- Jin, F.Y., et al., Secretory leukocyte protease inhibitor: a macrophage product induced by and antagonistic to bacterial lipopolysaccharide. *Cell*, 1997. 88(3): p. 417-26.
- Lu, B., et al., The acute phase response stimulates the expression of angiotensin-like protein 4. *Biochem Biophys Res Commun*, 2010. 391(4): p. 1737-41.
- Zhu, P., et al., Angiotensin-like 4: a decade of research. *Biosci Rep*, 2012. 32(3): p. 211-9.
- Pervushina, O., et al., Platelet factor 4/CXCL4 induces phagocytosis and the generation of reactive oxygen metabolites in mononuclear phagocytes independently of Gi protein activation or intracellular calcium transients. *J Immunol*, 2004. 173(3): p. 2060-7.

35. Bozoyan, L., et al., Interleukin-36gamma is expressed by neutrophils and can activate microglia, but has no role in experimental autoimmune encephalomyelitis. *J Neuroinflammation*, 2015. 12: p. 173.
36. Vigne, S., et al., IL-36R ligands are potent regulators of dendritic and T cells. *Blood*, 2011. 118(22): p. 5813-23.
37. Lee, M.S., et al., OASL1 inhibits translation of the type I interferon-regulating transcription factor IRF7. *Nat Immunol*, 2013. 14(4): p. 346-55.
38. Takaoka, A., et al., DAI (DLM-1/ZBP1) is a cytosolic DNA sensor and an activator of innate immune response. *Nature*, 2007. 448(7152): p. 501-5.
39. Pollpeter, D., et al., Impaired cellular responses to cytosolic DNA or infection with *Listeria monocytogenes* and vaccinia virus in the absence of the murine LGP2 protein. *PLoS One*, 2011. 6(4): p. e18842.
40. Arthur, J.C., et al., Cutting edge: NLRP12 controls dendritic and myeloid cell migration to affect contact hypersensitivity. *J Immunol*, 2010. 185(8): p. 4515-9.
41. Kim, B.H., et al., A family of IFN-gamma-inducible 65-kD GTPases protects against bacterial infection. *Science*, 2011. 332(6030): p. 717-21.
42. Shi, M., et al., TRIM30 alpha negatively regulates TLR-mediated NF-kappa B activation by targeting TAB2 and TAB3 for degradation. *Nat Immunol*, 2008. 9(4): p. 369-77.
43. Traves, P.G., et al., Pivotal role of protein tyrosine phosphatase 1B (PTP1B) in the macrophage response to pro-inflammatory and anti-inflammatory challenge. *Cell Death Dis*, 2014. 5: p. e1125.
44. Riley, J.P., et al., PARP-14 binds specific DNA sequences to promote Th2 cell gene expression. *PLoS One*, 2013. 8(12): p. e83127.
45. Cho, S.H., et al., B cell-intrinsic and -extrinsic regulation of antibody responses by PARP14, an intracellular (ADP-ribosyl)transferase. *J Immunol*, 2013. 191(6): p. 3169-78.
46. Lechmann, M., et al., The CD83 reporter mouse elucidates the activity of the CD83 promoter in B, T, and dendritic cell populations in vivo. *Proc Natl Acad Sci U S A*, 2008. 105(33): p. 11887-92.
47. Loscher, C.E., et al., Proinflammatory cytokines in the adverse systemic and neurologic effects associated with parenteral injection of a whole cell pertussis vaccine. *Ann N Y Acad Sci*, 1998. 856: p. 274-7.
48. O'Neill, L.A., How Toll-like receptors signal: what we know and what we don't know. *Curr Opin Immunol*, 2006. 18(1): p. 3-9.
49. Shi, Y., et al., Detoxification of endotoxin by aluminum hydroxide adjuvant. *Vaccine*, 2001. 19(13-14): p. 1747-52.
50. Bufe, B., et al., Recognition of bacterial signal peptides by mammalian formyl peptide receptors: a new mechanism for sensing pathogens. *J Biol Chem*, 2015. 290(12): p. 7369-87.
51. Fu, H., et al., Ligand recognition and activation of formyl peptide receptors in neutrophils. *J Leukoc Biol*, 2006. 79(2): p. 247-56.
52. Rajakariar, R., et al., Hematopoietic prostaglandin D2 synthase controls the onset and resolution of acute inflammation through PGD2 and 15-deoxyDelta12 14 PGJ2. *Proc Natl Acad Sci U S A*, 2007. 104(52): p. 20979-84.
53. Sato, M., et al., Positive feedback regulation of type I IFN genes by the IFN-inducible transcription factor IRF-7. *FEBS Lett*, 1998. 441(1): p. 106-10.
54. McNab, F., et al., Type I interferons in infectious disease. *Nat Rev Immunol*, 2015. 15(2): p. 87-103.
55. Huber, J.P. and J.D. Farrar, Regulation of effector and memory T-cell functions by type I interferon. *Immunology*, 2011. 132(4): p. 466-74.
56. Reynolds, J.M., et al., Toll-like receptor 2 signaling in CD4(+) T lymphocytes promotes T helper 17 responses and regulates the pathogenesis of autoimmune disease. *Immunity*, 2010. 32(5): p. 692-702.
57. Martin, S.W., et al., Pertactin-negative *Bordetella pertussis* strains: evidence for a possible selective advantage. *Clin Infect Dis*, 2015. 60(2): p. 223-7.
58. Lam, C., et al., Rapid increase in pertactin-deficient *Bordetella pertussis* isolates, Australia. *Emerg Infect Dis*, 2014. 20(4): p. 626-33.
59. Quintana, F.J., et al., Induction of IgG3 to LPS via Toll-like receptor 4 co-stimulation. *PLoS One*, 2008. 3(10): p. e3509.
60. Raeven, R.H.M., et al., Immunological signatures after *Bordetella pertussis* infection demonstrate importance of pulmonary innate immune cells. Manuscript submitted.
61. Zollinger, W.D., et al., Design and evaluation in mice of a broadly protective meningococcal group B native outer membrane vesicle vaccine. *Vaccine*, 2010.
62. Benjamini, Y. and Y. Hochberg, Controlling the false discovery rate: a practical and powerful approach to multiple testing. *Journal of the Royal Statistical Society*, 1995. 57(1): p. 289-300.
63. Samarajiwa, S.A., et al., INTERFEROME: the database of interferon regulated genes. *Nucleic Acids Res*, 2009. 37(Database issue): p. D852-7.

Supplementary information

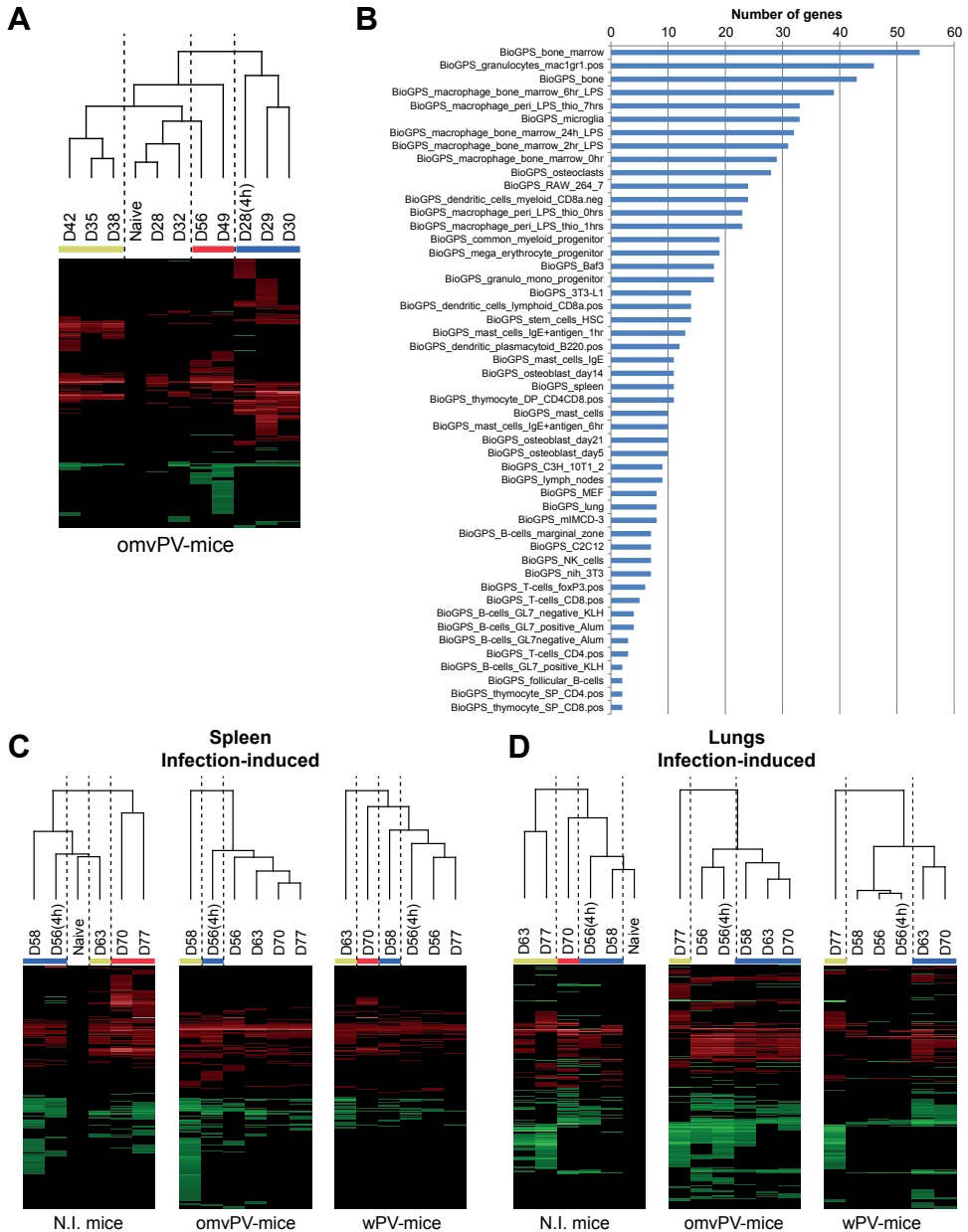


Figure S1 - Hierarchical clustering and BioGPS comparison of splenic transcriptome. (A) Hierarchical clustering of the omvPV-induced splenic transcriptome dataset to identify which time points showed a similar response. The response was divided in four parts illustrated by the different colors. **(B)** Transcriptomic profiles from spleen tissue of omvPV-mice and wPV-mice were compared with BioGPS databases. The numbers of genes detected in the different BioGPS databases are listed. **(C-D)** Hierarchical clustering on the **(C)** splenic and **(D)** pulmonary transcriptome datasets of challenged N.I.-mice, omvPV-mice and wPV-mice to identify which time points showed a similar response.

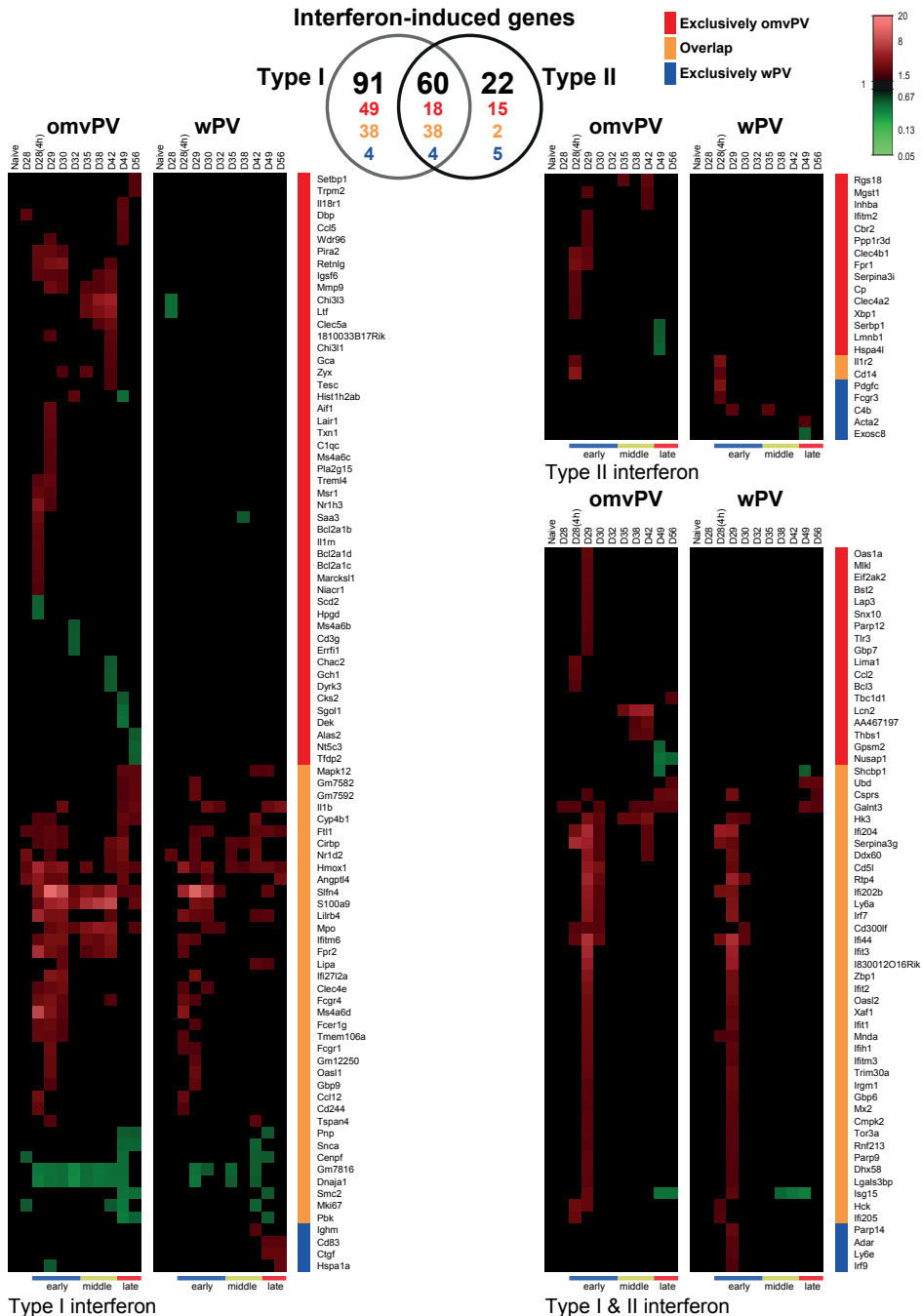


Figure S2 - IFN-induced genes in spleens of omvPV- and wPV-immunized mice. Genes induced by omvPV and wPV in the transcriptome of the spleen were matched with the Interferome database (<http://www.interferome.org/interferome/home.jspx>). A Venn diagram shows the total number of genes (black) induced by type I IFN, type II IFN, or both. Genes that were found exclusively in the omvPV-mice (red), wPV-mice (blue) or overlapped in both groups (orange) are depicted. The individual genes involved in type I IFN, type II IFN, or both are shown in heatmaps with the corresponding color codes of immunization background.

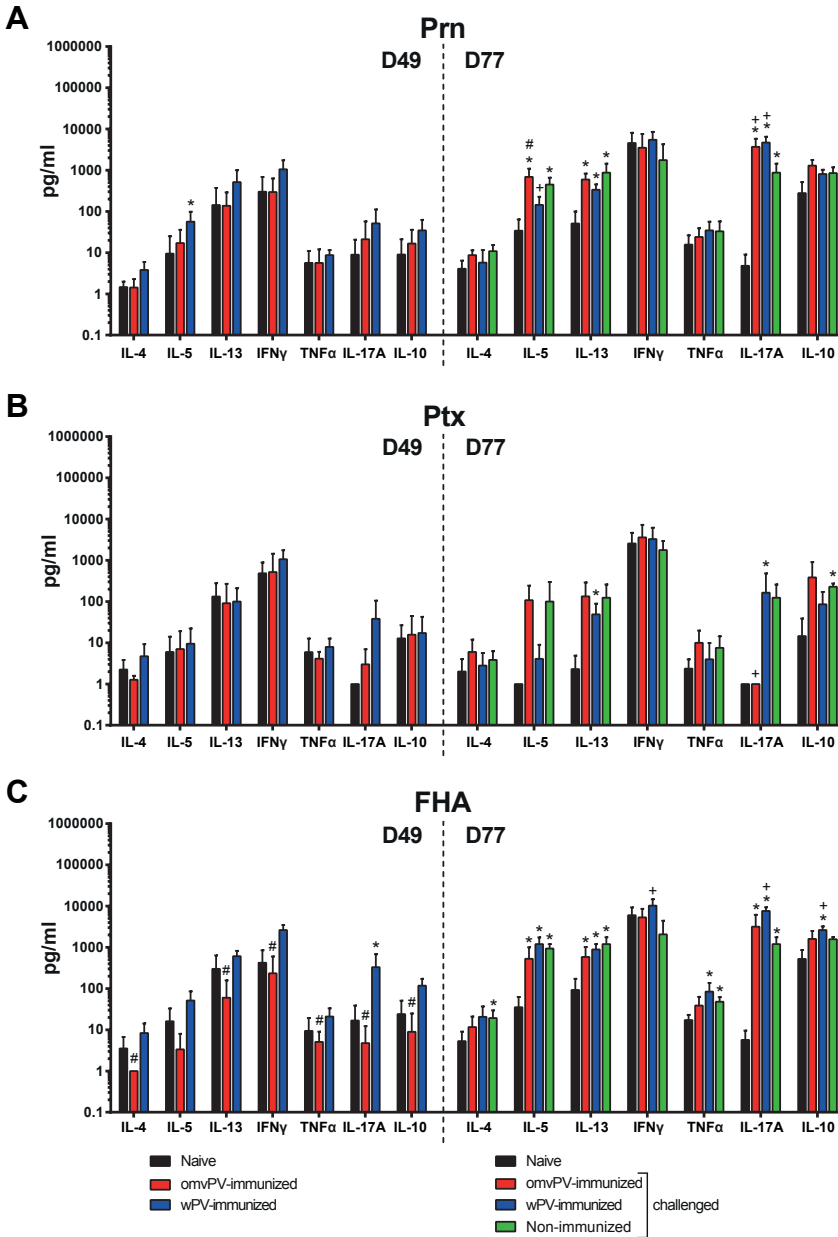


Figure S3 - Splenic cytokine responses after antigen restimulation in omvPV- and wPV-immunized mice before and after challenge as compared to naive control mice before and after challenge. (A-C) Concentrations of IL-4, IL-5, IL-13, IFN γ , TNF α , IL-17A and IL-10 were determined in the culture supernatants after 7 day stimulation of splenocytes with 1 μ g/ml **(A)** Prn, **(B)** Ptx, or **(C)** FHA. Splenocytes were harvested post booster immunization (day 49, left panel) of mice immunized with omvPV (red) or wPV (blue). Post-challenge (day 77, right panel), same groups were included with an additional group of non-immunized mice that received a challenge (green). In both experiments, complete naive mice (black) were used as control. Results for each mouse are corrected for medium stimulation. * = $p \leq 0.05$ for immunized group and challenged group vs. naive group, # = $p \leq 0.05$ for omvPV group vs. wPV group, + = $p \leq 0.05$ for challenged immunized group vs. challenge non-immunized group.

About the cover: The Devil's Throat of the Iguazu waterfalls seen from the Brazilian side. The world's biggest waterfall system divided over approximately 275 falls stretched over 2.7 km on the border between Brazil and Argentina. Part of the UNESCO World Heritage. In 2013, René attended the Keystone Symposium "*Advancing Vaccines in the Genomics Era*" that was held in Rio de Janeiro, Brazil.